# MICROSACCADE DISCONJUGACY DISTRIBUTIONS AND CHARACTERISTICS IN 2D VS 3D, ILLUSORY 3D, AND ACTIVE 3D DEPTH CONDITIONS

by
Yvette Tan

A thesis submitted to Johns Hopkins University in conformity with the requirements for the degree of Master of Science in Engineering

Johns Hopkins University
Baltimore, Maryland
August 2021

© 2021 Yvette Tan

All rights reserved

## ABSTRACT

Microsaccades are small, quick, fixational eye movements that share a neural pathway with saccades, and can offer a behavioral window into the state of different neural systems. Microsaccade studies generally involve fixation on 2D targets constrained to a flat plane, but with the lack of depth cues afforded by 2D targets and images, these studies may not fully demonstrate microsaccadic properties during viewing of real 3D targets at different depths. This thesis studies how microsaccade characteristics such as binocularity, amplitude, and rate change during viewing of 3D targets during depth-related tasks. Recent evidence has shown that the saccadic premotor pathways control the eyes separately, and thus microsaccade binocularity contains a significant proportion of disconjugate movements, where the two eyes have different amplitudes and directions (Cullen & Van Horn 2012; Gautier et al., 2017).

Here, I recorded movements from both eyes simultaneously and compared microsaccades generated to 2D and 3D targets that were viewed both near and far from the subject. Microsaccades were also recorded while subjects viewed two types of 2D images with 3D percepts, and lastly during the Brock string exercise, an active 3D task in vision therapy that involves focusing on beads placed at different distances away from the subject along a string. Simultaneous recordings were made using the standard scleral eye coil approach and a novel video-based system (VOG), which I developed as another means to track eye movements less-invasively. I found that binocularity and amplitude distributions were significantly different between near and far fixational conditions in 3D, as well as in 2D illusional depth and during the Brock string exercise. Noise levels were found to be 90% higher in VOG compared to eye coil data, therefore some differences in microsaccade characteristics found using the coil technique

did not reach significance in the VOG data. This result emphasizes that accurate characterization of microsaccades requires eye measurement techniques to have minimal noise.

Overall, my findings suggests that depth cues afford information that affects the behavior of microsaccade characteristics. Thus, my results have implications in understanding the binocularity aspects of microsaccades during visual tasks in 3D.

Supervisor: Dr. Kathleen E. Cullen

Readers: Dr. Charles Della Santina, Dr. Gene Fridman

## ACKNOWLEDGEMENTS

After arriving in Baltimore two years ago, just a few months out of my undergraduate biology degree, I often struggled to understand or get caught up with many of the engineering-related topics my classmates had prior exposure to. However, I was blessed to have met many wonderful friends and colleagues who helped make graduate school exciting and memorable even amidst the difficulties. I could not have done it without them.

First and foremost, I'd like to thank my advisor Dr. Kathleen Cullen, who took me into the lab and believed in me before I even knew what I was capable of. Thank you for the guidance and help you've given me over the past two years. Thank you also to my second readers, Dr. Charles Della Santina and Dr. Gene Fridman for all your constructive feedback on this thesis.

Thank you to everyone in the Cullen lab for all the help and support you've given me, truly this thesis was made possible through your help and suggestions. A huge thank you to our senior graduate student Omid Zobeiri, for being the first to make me feel welcome in the lab by chatting with me when we'd run into each other on the shuttle, and for patiently and willingly explaining a variety of different topics to me. I also am particularly grateful to Dale Roberts, our lab's technology expert, who played an important role in the eye coil experiments, and has taught me many electrical and software concepts. Thank you also to Ran and Vanessa, for keeping me updated on Asian entertainment news and in general for always being friends I can talk to and count on, to Aamna for all the encouragement and reassurance, to Liv for the help and ideas you've given me, and to Subhi for being a great assistant during the recording sessions.

A special thanks to my classmates turned friends, Tarana Kaovasia, Yvonne Chen, Molly Accord, Alysia Martin, Zina Kurian, and Hannah Comeau. Spending late nights in Brody studying would have been fruitless and depressing without you all.

Last but not least, thank you to my family and friends back home for the love and support I've received while pursuing this degree. I came here to challenge myself but your encouragement was a great comfort to me.

# TABLE OF CONTENTS

Abstract …….…….ii
Acknowledgements ……...….iv
List of Tables…….…….ix
List of Figures…….……..viii
Chapter 1: Introduction ……...1
1.1 Overview ……..1
1.2 Eye movements ……1
1.3 Saccadic burst neurons……...2
1.4 The superior colliculus and the saccadic pathway…….3
1.5 Microsaccades……4
1.6 Debates surrounding microsaccade characteristics and functions…….……5
1.7 Microsaccades in the context of binocular vision……..……7
1.8 2D and 3D targets in microsaccade studies……..…….8
1.9 Microsaccade conjugacy……..……..9
1.10 Control of disconjugate saccades and microsaccades……10
1.11 Research goals……..…...……..11
Chapter 2: Microsaccade disconjugacy distributions in 3D, Illusory 3D, and Active 3D Depth Conditions…….……12
2.1 Abstract……..……..12
2.2 Introduction……..12
2.3 Materials and Methods…….15
2.3.1 Subjects…….15
2.3.2 Video oculography system development…….…….15
2.3.3 Eye coils……...…….16
2.3.4 Experimental Design…….…...…….16
2.3.5 Microsaccade Detection……...…….17
2.3.6 Statistical Analysis……...…….19
2.4 Results……..20
2.4.1 Conjugate Characteristics…….20

2.4.2 Microsaccade Binocularity…….…….22
2.4.3 Comparison between Eye coils and VOG Systems……..23
2.5 Discussion……25
2.5.1 Summary of Results …….25
2.5.2 Microsaccades during 3D vs 2D viewing ……26
2.5.3 Microsaccades during fixation in 2D perceptual depth……27
2.5.4 Microsaccades during the Brock string exercise……..28
2.5.5 Binocularity Distributions in Microsaccades……29
2.5.6 Future Work……..30
Chapter 3: Discussion ……...31
3.1 Summary……..31
3.2 The VOG system…….…….31
3.3 Future Work…… 33
3.4 Conclusion.……..34
Tables ……35
Figures……38
References……..55
Supplementary Figure……62

## LIST OF TABLES

Table 1.1: Classes of eye movements

Table 2.1: Main sequence slopes

Table 2.2: Average Microsaccade rates

Table 2.3: Significant differences between binocularity during 2D vs 3D fixation

Table 2.4: Binocularity and Amplitude t-test comparisons

# LIST OF FIGURES

Figure 1.1: The Saccadic Pathway
Figure 1.2: Illusions used in microsaccade studies
Figure 1.3: Neural Control of Disconjugate saccades
Figure 1.4: Example velocity traces for conjugate and disconjugate microsaccades
Figure 1.5: Distribution of microsaccade binocularity
Figure 2.1: 3D convergence board sphere targets
Figure 2.2: The Magic Eye image
Figure 2.3: Spiral depth illusion
Figure 2.4: The brock string exercise
Figure 2.5: Example eye movement traces
Figure 2.6: Detection algorithm
Figure 2.7: Mean amplitudes of microsaccades across conditions
Figure 2.8: Main sequences during 2D and 3D fixations
Figure 2.9: Average microsaccade rates
Figure 2.10: Microsaccades during 2D vs 3D sphere tasks
Figure 2.11: Microsaccades during the Magic Eye depth illusion task
Figure 2.12: Microsaccades during the spiral depth illusion task
Figure 2.13: Microsaccades during the Brock string exercise task

# Chapter 1: INTRODUCTION

## 1.1 Overview

Eye movements are a critical part of our visual system, not only for taking in visual information but also for a variety of other functions such as directing attention, providing social cues, or even indicating the state of central and peripheral sensory systems such as in the vestibular system. Neurons from brain regions along the oculomotor pathways are involved in controlling 6 extraocular muscles for each eye: the medial and lateral rectus muscles controlling horizontal eye movements, and the superior and inferior rectus muscles and superior and inferior oblique muscles controlling vertical and torsional movements. These different oculomotor pathway neurons produce and modify a range of different eye movements that change how we focus on different aspects of our environment.

## 1.2 Eye movements

Visual system functions rely on a collection of eye movements which Raymond Dodge separated into 5 distinct classes of voluntary and involuntary movements (Dodge, 1903), summarized in *Table 1.1*. Voluntary eye movements include saccades, which are fast eye movements for redirecting gaze, smooth pursuit eye movements for tracking moving objects, and vergence movements for rotating the eyes while fixating at different depths. The involuntary eye movements are the vestibulo-ocular reflex (VOR) which keeps images stable while the head moves, and the optokinetic reflex which stabilizes vision during movement of peripheral targets (Cullen & Van Horn, 2011, p. 2). Microsaccades are small, fixational eye movements that are

saccadic and yet produced involuntarily, and therefore do not fall under only one class mentioned by Dodge. This thesis focuses on microsaccades, which will be expanded on below.

### 1.3 Saccadic Burst Neurons

Based on studies by Robinson and collaborators, driving saccadic eye movements requires a pulse or burst of action potentials by motoneurons to overcome the viscosity of the tissues surrounding the eye. This pulse of action potentials acts as a neural command signal for saccades, and is generated by saccadic burst neurons (SBNs) in the paramedian pontine reticular formation (PPRF) and mesencephalic reticular formation (MRF) (Figure 1.1). Firing by SBNs have been shown through first order modeling to encode saccade trajectories (Cullen and Guitton, 1997; Van Horn and Cullen, 2008; Van Horn et al., 2008), and to include the excitatory burst neurons (EBNs) from the rostral part of the PPRF and inhibitory burst neurons (IBNs) from the caudal pontine reticular formation. The firing of EBNs and IBNs precede saccade onset by about 10-20ms (Cullen and Guitton, 1997; Scudder et al., 1988). Excitatory long-lead burst neurons (eLLBNs) are another class of burst neurons found in the same areas as the EBNs and IBNs; however, their bursts are preceded by low frequency activity 16-200ms before the saccade (Munoz et al, 2000). As their name suggests, saccadic burst neurons do not seem to drive other eye movements such as smooth pursuit and slow vergence, and their firing duration and amount correlate to saccade durations as well as amplitude and peak velocity (Cullen and Guitton, 1997; Hepp and Henn, 1983; Keller, 1974; Luschei and Fuchs, 1972; Strassman et al., 1986a, 1986b; Van Gisbergen et al., 1981).

### 1.4 The Superior Colliculus and the Saccadic Pathway

Saccades are the fastest type of eye movements and can reach speeds of 900 degrees per second. Saccades begin in the superior colliculus (SC) in the midbrain, which takes input from widely distributed areas including the frontal eye fields, the posterior parietal cortex, and the basal ganglia (for a diagram of the saccadic pathway, see Figure 1.1). The SC is organized as a motor map for gaze control, with saccade direction and amplitude determined by the location of the initiating neuron population within the SC. The SC's motor map consists of a grid where iso-directional lines run rostral-caudally (front to back), and iso-amplitude lines run medial-laterally (from and away from the midline). Stimulation of increasingly caudal sites drives increasingly higher amplitude saccades, while stimulation increasingly further from the midline drives larger changes in saccade direction. Saccade trajectory is based on the average firing of a population of neurons in the SC rather than on the firing of a single neuron (Visuomotor Integration, Cullen, 2013).

Neurons in the superior colliculus send projections to numerous brainstem areas. To produce saccades, the main connections lead to the PPRF and the nucleus raphe pontis in the pons, as well as the MRF in the midbrain. Premotor SBNs in the PPRF drive horizontal saccades and project to the abducens nuclei both directly and through the nucleus prepositus (NPH). The abducens nerve controls the lateral rectus muscle, which is responsible for outward gaze shifts. In a parallel pathway, the premotor SBNs in the rostral interstitial MRF drive vertical saccades and project to the trochlear nerve (cranial nerve IV) both directly and through the interstitial nucleus of Cajal (INC), with the trochlear nuclei controlling the inferior and superior oblique muscles that are important in both vertical saccades as well as oblique/torsional saccades.

The PPRF and the INC both innervate the oculomotor nuclei, the axons of which (cranial nerve III) project to the medial, super and inferior rectus muscles, which as a group control saccades of all directions. Neurons in the NPH, the medial vestibular nuclei, and the INC give a step command based on the integration of the PPRF and MRF pulse signals, holding the eye in its new position after the saccade is over. Saccades can be prevented by signals from omnipause neurons (OPNs) in the nucleus raphe pontis in the pons, which send inhibitory projections to the PPRF and MRF burst neurons.

The VOR, which helps to stabilize gaze during head movements, usually involves an alternating pattern of eye movements called vestibular nystagmus. Nystagmus involves a slow compensatory phase and a quick resetting phase of eye movements, with the quick phase using the same neural pathway as that of the saccadic pathway (Harrison et al., 2015).

### 1.5 Microsaccades

During fixation, one might assume the eyes would remain still. However, there is constant motor activity in the extraocular muscles, producing microsaccades and other movements such as drift and tremor (Martinez-Conde at al., 2009). This thesis focuses on microsaccades, which are small, involuntary eye movements that occur during fixation. Microsaccades lie on the saccadic main sequence, and are produced through the same neural pathways (Hafed, Goffart, Krauzlis, 2009), although one key difference is that microsaccades are generated in the rostral part of the SC rather than the caudal. While research has found an interaction between microsaccades and different cognitive processes such as perception and attention, much remains unknown about what affects microsaccade characteristics and in turn how they may influence visual processing.

Microsaccades generally appear synchronously between the right and left eyes, and are thought to counteract visual fading (Martinez-Conde et al., 2006, McCamy et al., 2012) by re-foveating the target after intersaccadic drifts, as well as serving exploratory (Rucci, 2015), corrective (Cornsweet, 1956, Hafed, 2011, Otero-Millan et al, 2011), and perceptual (van Dam & van Ee, 2005) purposes. For example, they drive illusory motion in illusions such as the *Enigma* illusion (Troncoso et al., 2007) (Figure 1.2a) and the rotating snakes illusion (Otero-Millan et al., 2012) (Figure 1.2b). Microsaccade characteristics have been found to change with viewing targets and tasks (Gautier et al., 2016; Otero-Millan et al., 2008; McCamy et al, 2013), as well as with location of attention during fixation (Engbert, 2006, Engbert & Kliegl, 2003b; Hafed & Clark, 2002). For example, microsaccades were found to be larger and less frequent during fixation of larger and less precise targets (Steinman, 1965, McCamy et al., 2013), and are suppressed during high acuity tasks such as rifle shooting or needle threading (Winterston & Collewijn, 1976; Ko et al., 2010; Valsecchi & Gegenfurtner et al., 2014).

### 1.6 Debates surrounding microsaccade characteristics and functions

Several debates surround both the characteristics and functional aspects of microsaccades. Microsaccade detection criteria, for example, vary across group and study, with different upper amplitudes being employed for detection; older studies use 12 arcmin as an upper amplitude (Boyce, 1967; Ditchburn & Foley-Fisher, 1967; St. Cyr & Fender, 1969; Malinov, Epelboim, Herst, and Steinman, 2000;), while more recent studies use 1 degree (Engbert & Kliegl., 2004; Engbert, 2006b; McCamy et al., 2014), 1.5 degrees (Valsecchi et al., 2007; Kliegl et al., 2009; Privitera et al., 2014), and even 2 degrees (Martinez-Conde et al., 2006).

In discussions pertaining to functional aspects, many have questioned whether microsaccades serve a functional purpose. Of those who believe microsaccades lack a useful purpose (Kowler & Steinman, 1980, Collewijn, Kowler, 2008), reasons include that some studies have reported trained subjects could suppress their microsaccades (Fiorentini and Ercoles, 1966, Steinman et al., 1967) and that microsaccades are suppressed during high acuity tasks such as rifle shooting or needle threading (Kowler and Steinman, 1979, Winterson and Collewijn, 1976). Other reasons given include the suggestion that microsaccades result during artificial lab conditions (Malinov, Epelboim, Herst, & Steinman, 2000) and the finding that drifts are more effective than microsaccades in preventing visual fading (Gerrits & Vendrik, 1970).

However, these studies do not rule out a functional purpose for microsaccades. For example, while Winterson & Collewijn believed that the decrease in microsaccade rates during finely guided visuomotor tasks indicates microsaccades are unnecessary in completing such tasks, Bridgeman & Palca believed it to merely be a way to avoid missing information during the saccades. Therefore, there have been different implications or interpretations of the findings used as evidence by those who believe microsaccades to have no use. Debates about drift and flutter in comparison to microsaccades have generally faded out of recent microsaccade literature as it has become agreed that such movements act together during fixation. Microsaccades as small movements may also add useful positional jitter or noise to neuronal spike information about the retinal image position, creating a similar result to the linearization effect of noise in different sensory systems (Yu & Lewis, 1989).

### 1.7 Microsaccades in the context of binocular vision

To date, there are surprisingly few studies investigating the binocularity of microsaccades. Because everyday tasks involve looking at different depth levels, binocular oculomotor coordination is important for determining object and task positions. Saccades have been shown to coordinate binocularly (Malinov et al, 2000), but it is an open question whether microsaccades have a role in helping vergence during fixation. Microsaccades are thought to help correct fixational position as well as binocular disparity and vergence errors (Cornsweet, 1956, Engbert & Kliegl, 2004; Pérez Zapata, Aznar-Casanova, & Supèr, 2013; Valsecchi & Gegenfurtner, 2014; St. Cry & Fender, 1969; Krauskopf et al., 1960). Premotor neurons have also been shown to code integrated commands for vergence during microsaccades (Van Horn & Cullen, 2011). Though there have been some arguments that drift rather than microsaccades corrects binocular disparity (St.Cyr & Fender, 1969) and fixation position (Steinman et al., 1967), microsaccades have been found to work with drift to correct fixation position and disparity (Cornsweet, 1956; Krauskopf et al., 1960; Engbert & Kliegl, 2004). Valsecchi and Gegenfurtner, 2014 studied microsaccades while subjects made saccades along a slanted plane and found that the change in vergence angle was consistent with the horizontal direction of the microsaccades, meaning that microsaccades may help to control for vergence as well as change in amplitude depending on task. Valsecchi and Gegenfutners' study in particular employed "gaze in depth" vectors as a way to analyze microsaccades moving with respect to depth. However, there have been mixed results as to whether microsaccades help to correct vergence error. For example, microsaccades that occurred after a large saccade were found to correct vergence error caused by a pictorial cue (Pérez Zapata, Aznar-Casanova, and Supèr, 2013), but other studies

have shown that microsaccades provide no change in vergence during tasks with pursuits in depth (Richter and Engbert, 2013).

### 1.8 2D and 3D Targets in microsaccade studies

In addition to a lack of binocularity studies, the microsaccade literature often fails to utilize 3D tasks or targets. Perhaps due to ease of changing targets and intersperse different attentional cues, targets, or distractions, most studies use 2-dimensional targets displayed on a screen. Of the few paradigms using 3D targets, LEDs have been a prime target choice whether for non-human primate studies (Van Horn & Cullen, 2011) or human studies (Epelboim et al, 1997; Aytekin et al., 2013; Fang et al., 2018). High-precision acuity tasks comprise some of the few other tasks that involve depth cues for the participant. These include needle threading and air rifle firing (Winterson & Collewijn, 1976), determination of electrode tip position (Bridgeman & Palca, 1980), as well as a more recent study having participants position a needle tip on the corner of a target plate (Valsecchi and Gegenfurtner, 2014). In regard to their relationship with depth, microsaccades have been recorded during the tapping of objects at different depths (Epelboim et al, 1995), and during fixation between marks 2 to 5mm in distance on a slanted plane (Valsecchi and Gegenfurtner, 2014), though the later were actually microsaccade sized instructed saccades. Though some of these studies have employed such depth related tasks or 3D targets, there is more to study in terms of the depth cues available in a display as well as the visual properties of the display and tasks. One topic this thesis considers is how a 3D target or the presence of depth cues may affect microsaccade characteristics as compared with 2D targets or views.

### 1.9 Microsaccade Conjugacy

One of the larger debates regarding microsaccades involves their binocular characteristics. In particular, the Hering-Helmholtz Binocular Control debate between two German physiologists in the 1800s focuses on the neurophysiological basis for binocular eye control. Ewald Hering believed that we are born able to move our eyes in coordination, and his 'law of equal innervation' states that the eye muscles are equally innervated, providing for coordinated or conjugate movements in the eyes. Hermann von Helmholtz, in contrast, believed that the brain is initially wired to allow the eyes to move independently, and that we learn over time to move them together. This is illustrated in Figure 1.3.

Classically, microsaccades were thought to be strictly conjugate (Krauskopf et al., 1960, Møller et al., 2002, Nyström et al., 2017, Fang, Gill, Polette, & Rucci, 2018), meaning that they appear synchronously in both eyes with the same amplitude and direction, and follow Hering's law. However, there is evidence for the encoding of disconjugate microsaccades, in which microsaccades may happen monocularly or in which the amplitudes and directions of microsaccades may not match in the right and left eyes. Eye tracking in conjunction with neural recordings in monkeys during fixation has shown that the brain controls the movement of each eye individually (Van Horn & Cullen, 2011), which disproves Hering's law, and has found disconjugate movements in more than half of the study's detected microsaccades (Figure 1.4, 1.5). The neural basis of microsaccades determined in non-human-primate studies such as Hafed et al., 2009 and Van Horn & Cullen, 2011 allows for a distribution of disconjugate movements in microsaccades, which could function to correct vergence or binocular disparity.

### 1.10 Control of disconjugate saccades and microsaccades

The movement of each eye is encoded separately through multiple neurons and steps in the saccadic premotor pathway, rather than by specific conjugate and vergence commands (Cova & Galiana, 1995; King & Zhou, 2002; Sylvestre & Cullen, 2002; Sylvestre et al., 2003; Van Horn & Cullen, 2009). Cullen & Van Horn, 2012 analyzed SBN firing during conjugate and disconjugate saccades and showed that 1. Firing of excitatory and inhibitory SBNs synchronize facilitated vergence, and SBNs fire during disconjugate saccades but not during slow vergence, 2. The majority of SBNs encode movement of one eye and not conjugate eye velocity (Figure 1.3), 3. Computer simulations demonstrated that premotor saccadic circuitry provides the vergence drive to the abducens motoneurons (Van Horn et al., 2008), and that 4. Horizontal SBNs respond during vertical-facilitated vergence but little during vertical conjugate saccades (Van Horn & Cullen, 2008). These findings suggest that premotor SBNs control the driving of disconjugate saccades.

Additional input is required in the saccadic premotor pathway to allow for conjugate movements as well as slow vergence. Conjugate movements are made possible by the medial longitudinal fasciculus (MLF), which consists of axons connecting the oculomotor nerve, trochlear nerve, and the abducens nerve. The MLF connects the interneurons of the abducens nucleus with the contralateral oculomotor nucleus motoneurons, as well as the vestibular nuclei with the oculomotor and trochlear nuclei and the interstitial nucleus of Cajal (Waitzman & Oliver, 2002). This allows for synchrony across the different eye muscles. While SBNs encode for disconjugate saccades, they do not fire during slow vergence. Slow vergence requires input from the central mesencephalic reticular formation, in which near-response neurons that project

to the medial rectus motoneurons were found to fire proportionally to vergence angle, and to be silent during conjugate saccades (Mays, 1984; Judge & Cumming, 1986; Zhang et al., 1992).

This physiological evidence for disconjugate control in saccades provides a background for the mechanism of disconjugate movements in microsaccades. However. it remains a question as to how this disconjugacy or binocularity distribution came to be and what it may be affected by. This thesis investigates how the disconjugacy distribution and other microsaccade characteristics such as amplitude distributions, main sequence slopes, and rate are influenced by the presence or absence of visual depth cues.

### 1.11 Research Goals

In this thesis, I explore how microsaccade binocularity, as well as amplitude, main sequence slopes, and rate are affected by depth in conditions of 1). 3D vs 2D depth, 2). Illusional depth, and 3). Active 3D depth.

While eye coils are the gold standard in eye movement recordings, their invasive nature has spurred work using video oculography (VOG) systems as an alternative. Contemporary, state-of-the art video trackers have already been shown to detect microsaccades in substantial agreement with scleral eye coils (McCamy et al., 2015). In this thesis, eye movements in humans were recorded using a newly developed video tracking system in conjunction with eye coils in order to validate the VOG system's suitability for studying microsaccades using non-invasive eye tracking in the future.

# Chapter 2: Microsaccade Disconjugacy Distributions and Characteristics in 2D vs 3D, Illusory 3D, and Active 3D Depth Conditions

## 2.1 Abstract

Microsaccades have been found to occur monocularly as well as in a distribution of disconjugate movements. In most microsaccade studies, however, they are studied using targets displayed on a 2D plane, lacking the depth cues available in the normal day-to-day visual world. In this study, I investigated how microsaccade characteristics, in particular their degree of disconjugacy, change between fixation on "near" and "far" targets in different depth contexts using 2D, 3D, and depth illusion targets. Distributions of disconjugacy varied significantly between 2D and 3D target fixation for both near and far, as well as between near and far conditions for paradigms in each type of depth context.

## 2.2 Introduction

Saccadic eye movements are an important behavioral window into the state of different neural systems, and their connection to microsaccades by neural pathways means that microsaccades may offer similar readouts of the brain's internal state. Microsaccades, which are small, involuntary eye movements that occur during fixation, are believed to play important roles in functions such as counteracting visual fading (Martinez-Conde et al., 2006, McCamy et al., 2012), providing corrective (Cornsweet, 1956, Hafed, 2011, Otero-Millan et al, 2011), and exploratory movements (Rucci, 2015), as well as driving perceptual (van Dam & van Ee, 2005)

changes. It is known that microsaccade characteristics are affected by viewing targets and tasks (Gautier et al., 2016; Otero-Millan et al., 2008; McCamy et al, 2013) as well as by location of attention during fixation (Engbert, 2006, Engbert & Kliegl, 2003b; Hafed & Clark, 2002), however there remains more to be discovered as to how and why microsaccades are produced.

Studies have now shown that the saccadic pathway allows for control of each eye individually rather than through conjugate and vergence commands (Cova & Galiana, 1995; King & Zhou, 2002; Sylvestre & Cullen, 2002; Sylvestre et al., 2003; Van Horn & Cullen, 2009), a finding that can be reasonably extrapolated to the conjugacy of microsaccades. Microsaccades recorded when monkeys fixated on LEDs at different distances showed a conjugacy-disconjugacy distribution (Cullen and Van Horn, 2012). Investigating how this distribution changes with different targets may offer key insight into perception and other visual coding processes. Surprisingly however, most studies only consider microsaccades that are synchronous and conjugate, which leaves more to be discovered about their disconjugate properties. Along with the lack of disconjugate-focused microsaccade studies is the lack of studies employing targets and tasks that are 3D in nature, as the majority of the microsaccade literature presents targets in 2D, usually on a screen. With the lack of depth cues afforded by 2D targets and images, eye movements recorded under these conditions may not accurately reflect microsaccade characteristics during viewing of real-world targets. Comparison of microsaccade characteristics during 2D versus 3D target fixation may therefore shed light on how depth cues affect these small eye movements.

This study aims to take a deeper look into the conjugacy-disconjugacy distribution of microsaccades, and to examine whether the distribution and other microsaccade characteristics are affected by factors related to depth. First, I compared microsaccades generated during fixation on 3D spheres placed at 15cm (“near”) and 90cm (“far”) away from the subject. For comparison as a

control paradigm, subjects also viewed a 2D representation of these same spheres in which each sphere subtended the same angle on the retina (Figure 2.1). Second, I compared microsaccades while subjects viewed two types of 2D images constructed to produce 3D percepts – a 'Magic Eye' image that requires convergence to see a hidden 3D donut (Figure 2.2), and an spiral illusory depth pattern (Figure 2.3). The conjugacy and disconjugacy of microsaccades was compared while subjects viewed the near versus far aspects of the illusions. Third and finally, I recorded eye movements while subjects performed the Brock string exercise, which is an active 3D task in vision therapy that involves focusing on beads placed at different distances away from the subject along a string (Figure 2.4). In this exercise, subjects perceive two crossing strings as they fixate on each bead, and are instructed to adjust their gaze such that the strings cross perceptually in or at the bead. Vision therapy techniques such as the Brock string exercise have been shown to improve visual strategies and conditions such as convergence insufficiency and visual accommodation (Maxwell, Tong & Schor, 2012; Jang et al., 2017; Wong et al., 2021), and this exercise in particular provides visual and oculomotor feedback, helping users improve their convergence.

In this study, an eye coil system was used to record eye movements in subjects. I also developed a new video oculography (VOG) system for non-invasively tracking eye movements in humans. As the eye coil system is the gold standard for eye tracking, binocular eye movements collected simultaneously from both systems were compared to evaluate if the quality of tracking by this new VOG system was sufficient for detecting microsaccades when compared to those detected in eye coil recordings.

I hypothesized that binocularity distributions would be significantly different between fixation of targets at different 3D depths, but not at depths represented in 2D. I further hypothesized

the same differences in microsaccade characteristics at different static 3D depths would be found in the more dynamic Brock string exercise.

My results demonstrate that 1). The binocularity and amplitude distributions, as well as the main sequence slopes, of microsaccades show significant differences between near and far 3D target fixation, but not of 2D control targets. 2). Binocularity distributions, amplitudes, and main sequence slopes also show significant differences between near and far target fixation of certain 2D illusional depth images, specifically the spiral illusion. 3). Microsaccade binocularity, amplitudes, and main sequence slopes are also different between near versus far Brock bead fixation.

## 2.3 Materials and Methods

### 2.3.1 Subjects

Eight subjects participated in 60 minute long recording sessions. All subjects had normal vision or wore eyeglasses to correct to normal and were assumed to have normal oculomotor function. All paradigms show data from all eight subjects, except the depth illusion paradigm and the 3D sphere paradigm eye, which have data from seven of the participants.

### 2.3.2 Video oculography system development

A new video oculography (VOG) system was constructed for eye movement tracking. FLIR Blackfly cameras, model BFS-U3-13Y3M-C, were used along with Tamron C-Mount Lenses for eye recordings. In order to limit noise from visible light, infrared pass filters were

attached to camera lenses. Infrared LED arrays were used to illuminate subjects' eyes to provide a constant source of light.

The VOG system was used in conjunction with the eye coil system by mounting the cameras and IR LED arrays to a pole with a bite bar, supported by a set of poles on either side of the patient's chair.

### 2.3.3 Eye coils

Data from scleral eye coils were sampled at 1000Hz. To limit discomfort, eye coils were left in place for a maximum of 60 minutes. Proparacaine eye drops were used as an anesthetic before eye coil placement, and fluorescein strips were used after the eye coils were taken out to check for scratches in the eyes.

### 2.3.4 Experimental Design

Subjects were head restrained by a bite bar while eye position was acquired by scleral eye coils at 1000 Hz in concurrence with a VOG system at 500 Hz, as described above.

I tested three types of paradigms, with five in total. The first paradigm was the convergence board, which consisted of spheres placed along the subject's midline at 15cm (near) and 90cm (far) away on a clear plastic board. Subjects alternated between focusing on near and far sphere targets in intervals of 5 seconds for 5 minutes. Near and far targets were molded so that their retinal image sizes were the same.

The second paradigm required the same task but instead in 2D with a picture of the spheres as a control against the 3D condition. The next set of paradigms involved 2D depth illusions, which consisted of a 'Magic Eye' image, and a spiral depth illusion pattern. In the Magic Eye image

condition, participants were instructed to converge their eyes in order to see a hidden 3D donut image, and to raise their hand when the donut was visible. When possible, the participant alternated between fixation on apparently "near" and "far" sections of the donut for 4 minutes total. For the second depth illusion paradigm, a spiral checkerboard depth illusion was displayed, and participants fixated alternatively for 5 seconds each over 4 minutes on areas of the picture which seemed "near" and "far".

The last paradigm was an active 3D task called the Brock string exercise, which is a vision therapy technique for the purpose of improving convergence. Participants fixated on beads along a string at distances of 6, 18 and 24 inches away for 20 seconds each. During the Brock string exercise, binocular vision makes the single string appear as two, and subjects adjust their gaze such that the strings are perceived to cross in or at the desired bead.

Several calibration trials were interspersed with these paradigms. These involved vertical and horizontal fixations on LEDs placed along a wall 122cm away at 5 degree increments from -20 to 20 degrees.

### 2.3.5 Microsaccade Detection

Data were separated by specific targets being fixated on, and by "near" or "far" fixation depending on the task. Eye traces were first manually inspected to ensure microsaccades were not mislabeled or missed. Eye movements were analyzed in conjugate coordinates, where

$$\text{conjugate} = (\text{left eye} + \text{right eye})/2.$$

A binocularity index was calculated in order to determine the degree of disconjugacy for each microsaccade, and was calculated as

$$I_{bino} = \left[max\left(\dot{E}_l\right) - max\left(\dot{E}_r\right)\right]/\left[max\left(\dot{E}_l\right) + max\left(\dot{E}_r\right)\right]$$

with $\dot{E}_l$ and $\dot{E}_r$ as the left and right eye velocities respectively. A binocularity index near 0 signifies a more conjugate movement, while increasingly positive indexes indicate higher left eye amplitudes compared to right, and increasingly negative indexes mean a higher right eye amplitude compared to left.

Data processing and microsaccade detection were based on algorithms used in Engbert & Kliegl, 2003. After data acquisition, left and right eye horizontal and vertical traces were independently processed and filtered at a cut-off frequency of 50 Hz. After filtering, the eye position time series were differentiated with a moving average of velocities over 5 data samples to suppress noise.

$$\overrightarrow{v_n} = \frac{\overrightarrow{x_{n+2}} + \overrightarrow{x_{n+1}} + \overrightarrow{x_{n-1}} + \overrightarrow{x_{n-2}}}{6\Delta t}$$

A velocity threshold was computed based on the median estimator of the velocity time series using the equation,

$$\sigma_{x,y} = \langle v_{x,y}^2 \rangle - \langle v_{x,y} \rangle^2$$

for both horizontal and vertical velocity components, in which the standard deviation of the velocity time series was multiplied by $\lambda = 7$ to give the horizontal and vertical thresholds $\eta_x$and $\eta_y$.

$$\eta_{x,y} = \lambda \sigma_{x,y}$$

Given the observed range of eye and therefore microsaccade velocities across different subjects and tasks, horizontal and vertical thresholds were quite low in some trace data, resulting in detected microsaccades that were found to be noise when visualized in eye position traces. Thus, in order to provide a clear standard for detection, a minimum velocity threshold of at least 5 degrees per

second was set. If the threshold provided through the calculations above was above 5 deg/s, then the calculated threshold was used for microsaccade detection.

The horizontal and vertical thresholds were used to create an elliptical threshold when plotting the x and y velocity planes, as shown in the top row figures of Figure 2.6. Data points in the velocity time series were labelled as microsaccades using this velocity threshold, and local maxima and minima were identified in order to separate microsaccades from one another. Additional detection criteria were included based on existing literature, such as making sure microsaccade durations were between 10-300ms (Fang et al., 2018) and that intersaccadic distances were at least 20ms (Martinez-Conde group). Microsaccades are visualized in example position traces in the bottom row of Figure 2.6.

### 2.3.6 Statistical Analysis

Microsaccades were first detected separately for both left and right eyes, and then combined for analysis. Microsaccade characteristics of binocularity, amplitude, main sequence slope, and rate were analyzed. Binocularity of microsaccades was analyzed by means of the binocularity index, which takes into account the peak velocities of the microsaccades in the right and left eye and provides a level of conjugacy for each microsaccade. Evaluated collectively for each fixation condition by combining the microsaccades across subjects, the microsaccade binocularity indices provide a distribution of the binocularity of eye movements during fixation of different targets. This binocularity distribution was found for each paradigm's near and far condition and was compared across paradigms and between near and far conditions.

Microsaccade amplitudes and main sequences (amplitude against peak velocity) were analyzed from conjugate traces rather than separate left and right eyes to give a more holistic picture

of these characteristics. In order to determine whether the slopes of the main sequences were significantly different between near and far conditions, each experimental paradigm's pair of near and far main sequences were fitted to a line by least squares, and the slopes were compared using an f-test. Two-tailed t-tests were used to compare whether there were significant differences in binocularity distributions and in amplitudes between "near" and "far" conditions, as well between 2D and 3D convergence board conditions. One-way ANOVAs allowed for comparing the distributions of "near" and "far" fixation between each of the five different experimental paradigms.

Microsaccade rate was calculated as simply the combined number of microsaccades detected in the left and right eyes over the amount of time the subjects fixated on the target.

## 2.4 RESULTS

In this study, I analyzed microsaccade characteristics during various depth related viewing paradigms. These characteristics include the conjugate amplitudes, binocularity distributions, main sequence slopes, and microsaccade rates.

### 2.4.1 Conjugate Characteristics

Amplitude characteristics of microsaccades can be affected by the requirements of a task as well as specific features of the fixation target (Steinman, 1965, Martinez-Conde et al., 2006;Valsecchi & Gegenfurtner, 2014; Amit et al., 2019). Accordingly, I first quantified amplitude distributions from the conjugate signals ( $\frac{left\ eye\ position + right\ eye\ position}{2}$) across paradigms and

compared them using two-tailed t-tests. Specifically, I compared amplitudes of near vs far and eye coil vs VOG for each paradigm, and then compared amplitudes between paradigms.

When analyzing eye coil recordings, the results show significant differences between amplitude distributions of near and far fixation during the 3D sphere, spiral depth illusion, and brock string paradigms (Figure 2.7; Table 2.4). The VOG recordings similarly show significant differences between the amplitudes of near and far fixation during the 3D sphere and Brock string paradigms. When comparing the amplitudes of paradigms between the data of our VOG and eye coil recording systems, I found significant differences between the majority of distributions. Due to this, I focus on characteristics given by microsaccades recorded by the eye coils.

A secondary analysis was done comparing microsaccade amplitudes across all paradigms, in which an ANOVA revealed differences in amplitude distributions between most of the paradigms. In the far condition, statistical differences in amplitudes were found in microsaccades between the 3D spheres and all other conditions as well as between the Magic Eye and all other conditions. In the near condition, the Magic Eye was again found to be statistically different from all other paradigms, while the 3D spheres and the Brock string paradigms showed significant amplitude differences with all paradigms except for one other.

Main sequences (Figure 2.8, Table 2.1) were first found to be consistent with previous studies, in that microsaccade amplitudes were proportional to peak velocities. Slopes between paradigms were quite comparable and fell within a range of 23.84 to 30.08. F-tests were used to compare the regression line slopes between the near and far main sequences for each condition. Significant differences were found in all paradigms except that of the Magic Eye. The f-test values are much higher in the 3D sphere and spiral depth illusion comparisons, suggesting

greater likeliness of significant difference between the slopes of the near and far regression lines in those paradigms.

Lastly, I compared microsaccade rates between the paradigms as the number of microsaccades over fixation duration (Figure 2.9, Table 2.2). Microsaccades appeared at average rates between 1 to 2 microsaccades per second for all paradigms and both depth fixation distances. Rates varied between subjects, e.g. rates across subjects during fixation of near 3D convergence board targets range from 1.14 to 2.02, 2D convergence board targets .30 to 1.59, depth illusion 0.24 to 1.96, Magic Eye .64 to 1.73, and brock string exercise .83 to 1.51. A one-way ANOVA analysis was performed between the rates of the different paradigms and displayed no significant differences for both near (P = .755) and far (P = .783) conditions.

### 2.4.2 Microsaccade Binocularity

My main focus was on the degree of disconjugacy of microsaccades, particularly between different fixational depths and between 3D vs 2D conditions. Modeling the study of microsaccade binocularity such as Cullen and Van Horn, 2012, I found a distribution of disconjugate movements between the left and right eyes, quantified by the binocularity index $I_{bino}$ calculated for each microsaccade. To compare these distributions across different parameters, I utilized two-tailed t-tests on binocularity indexes to understand whether there was a significant difference between distributions that occur during different fixation or task conditions.

First I compared eye movements for near and far targets between the 3D and 2D sphere paradigms. These t-tests on microsaccade binocularity indices in coil recordings showed significant differences between the 3D and 2D conditions during near target fixation, but not during far target fixation (Table 2.3). In comparing the binocularity distributions for coil-

recorded near and far conditions for the rest of the experimental paradigms, I found significant differences between near and far fixation for the 3D spheres, spiral depth illusion, and Brock string paradigms (Table 2.4). Comparing the near and far fixations of the experimental paradigms in the VOG recordings, I find generally the same results as the eye coil recordings, except a lack of significant difference in the spiral illusion paradigm. In viewing the proportions of microsaccades of different binocularities, as expected, I find that the majority are conjugate, with small fractions of disconjugate microsaccades (Figures 2.10-2.13). I also found that disconjugate microsaccades are skewed toward larger left eye peak velocities compared to the right eye, seen in the binocularity index distributions shown in graphs C and D of figures 2.10 through 2.13, where a binocularity index above 0 indicates a greater left eye movement, and below 0 indicates a greater right eye movement. Tables 2.3 and 2.4 p-values where <.05 signifies rejection of the null. Lastly, a one-way ANOVA showed that there are statistical differences between the binocularity distributions of the paradigms for both near ($P = .0467$) and far ($P = .010$) conditions. Comparing between paradigms with ANOVA, significant differences in binocularity were found between the far conditions of the 3D spheres against both the far Magic Eye ($P = .0111$) and the far spiral illusion (.0287), and between the near Magic Eye and near Brock string ($P = .036$) paradigms.

### 2.4.3 Comparison between Eye coils and VOG Systems

The new VOG system in this study was developed as another means to track eye movements non-invasively. As a way to evaluate how well the VOG system fared against the eye coil system, I compared binocularity and amplitudes of various conditions between and amongst VOG and coil recorded microsaccades. The binocularity and amplitude comparisons in Table 2.4 between near

and far demonstrate that many of the statistical differences carry over between eye coil and VOG detected microsaccades. However, while the VOG works well in some cases, it does seem to miss some aspects of microsaccades that can be pulled out with coils. For example, I also applied the two-tailed t-tests on the binocularity index distributions for near and far conditions between coil and VOG detected microsaccades for each paradigm. This gave significant differences in the far 3D ($P = .010$) and 2D ($P = .003$) convergence board and Magic Eye ($P = .009$) as well as near brock string ($P = .0113$) and spiral illusion ($P < .0001$) paradigms. The presence of such differences in the binocularity distributions of the microsaccades found between coil data and VOG data implies variability in eye tracking consistency for our VOG system.

In visualizing the traces between VOG and eye coil recordings (Figure 2.5), VOG traces generally mirror eye coil traces, but display much more drift and noise. Spatial noise for the two systems was calculated by averaging the baseline peak to peak noise in the eye coil and VOG traces in the first few seconds of each subject's calibration, and was found to be .23±.08 degrees for the VOG system compared to.02±.01 degrees for the eye coils. VOG noise levels, being 90% higher than coil noise levels, may not afford accurate detection of microsaccades, as high noise amplitudes can hide or obstruct the small eye movements in recordings. This would subsequently affect the characteristics of microsaccades recorded by the VOG system and lower the accuracy of statistical measurements made between such characteristics.

Some traces show great potential for this VOG system, as seen in Figure 2.5D, where the left eye coil and VOG traces are overlayed. Using left eye traces from the 3D sphere paradigm, an average variance accounted for (VAF) was calculated across all subjects to be .86±.15, revealing a high correlation between the two systems. However while the VAF suggests that these VOG recordings provide a decent estimate of the coil recordings, the differences in significance found in

microsaccade characteristics using eye coils versus VOG conveys that the high noise levels of the VOG system are inadequate for properly recording microsaccades. Thus, as eye coils are the gold standard of eye tracking, moving forward the discussion pertains to the data set obtained with the eye coils.

## 2.5 DISCUSSION

### 2.5.1 Summary of Results

The aims of this thesis were: 1) To examine the binocular conjugacy-disconjugacy distribution of microsaccades during fixation of near and far sphere targets in 3D and in a control, a 2D image of the targets. 2) To inspect these microsaccade characteristics during fixation of near and far in 2D images with the perception of depth. And 3) lastly compare these results with a comparable analysis of microsaccades during the Brock string exercise, a vision therapy exercise for improving convergence.

To date, the majority of studies that investigated microsaccades have defined microsaccades as strictly conjugate events. Indeed, Engbert & Kliegl, 2003's original microsaccade detection algorithm requires the rejection of monocular microsaccades. However, disconjugate microsaccades are evidenced both by eye movement recordings and neural pathways. Accordingly, here I recorded microsaccades in human subjects during different depth related 2D and 3D fixational and convergence tasks to see how binocularity might be affected by depth.

Overall, I found disconjugate movements in the microsaccades I recorded. In addition, to analyzing their degrees of disconjugacy, I quantified the conjugate amplitudes, main sequence

slopes, and rates of microsaccades made at different fixation viewing differences. Binocularity distributions, amplitude distributions, and main sequence slopes were significantly different between near and far sphere fixations in the 3D convergence board task. When comparing microsaccade characteristics between the 3D spheres and their 2D control image, near conditions showed differences in both binocularity and amplitude, while far conditions showed significant differences in only amplitude. Significant differences were also found between microsaccades in the near and far conditions of the same three characteristics in the spiral depth illusion paradigm and the brock string exercise.

### 2.5.2 Microsaccades during 3D vs 2D viewing

While most studies use 2D fixational targets and tasks in recording microsaccades, 2D tasks lack the depth cues afforded in everyday activities. Therefore microsaccades in these tasks may not have the same characteristics as those made to actual real world targets. Like Gautier et al., 2016, I found disconjugate microsaccades in humans, though Gautier et al.'s tasks focused on discrimination in comparison to fixation. I also found the degree of disconjugacy in microsaccades to change between near and far sphere fixations (Table 2.4), as well as between the near target 3D and 2D (Table 2.3).

With the differences in this binocularity, or coordination between the two eyes, my original hypothesis holds that there would be differences in microsaccades during near and far target fixations, due to the presence of depth information. It is interesting, however, that my findings regarding microsaccade binocularity distributions in humans differed in comparison with another recent study of disconjugacy in nonhuman primates. In particular, Van Horn & Cullen, 2011 studied microsaccades in rhesus monkeys during fixation of near and far LEDs, and found binocularity

distributions to be comparable rather than different in both near and far viewing, and disconjugate microsaccades to be in higher proportions than I found in the present study. As the literature concerning binocularity in microsaccades is quite sparse, more research is needed to better understand how depth information as well as other characteristics of a fixation task may affect microsaccade disconjugacy. Overall, my results suggest that depth affords information to the brain that affects the binocularity and amplitudes of microsaccades.

### 2.5.3 Microsaccades during fixation in 2D perceptual depth

In comparison to the sphere targets in real 3D, I decided to investigate how the perception of depth in the lack of real depth might affect microsaccade characteristics using two different images. In the first, subjects were instructed to produce the perception of a hidden 3D donut in a Magic Eye image (Figure 2.2) by holding their eyes in a converged state and fixating between near and far aspects of the donut. In the second, subjects were instructed to fixate between near and far looking areas in a spiral depth illusion (Figure 2.3). Microsaccade binocularity distributions were found to significantly differ between near and far fixations of the spiral illusion. This suggests that depth illusions afford information to the eyes similar to the depth cues in 3D. Given the differences in microsaccade characteristics in the spiral illusion, I expected to see differences in the Magic Eye paradigm as well. However, microsaccades were not statistically different in any characteristic distribution for the Magic Eye task in near and far conditions. Microsaccade rates during Magic Eye viewing were also generally the lowest compared to other paradigms, with near and far rates at 1.13 and 1.17 microsaccades/second respectively. The lower overall microsaccade rates and the lack of significant difference between microsaccade binocularity and amplitudes in near and far fixation of the Magic Eye task may be due to the active motor and cognitive tasks of holding the

eyes in a partially converged state to perceive the hidden 3D image, as well as due to the reduced precision of target points in the task.

### 2.5.4: Microsaccades during the Brock string exercise

My last paradigm was the Brock string exercise (Figure 2.4), a vision therapy technique in which subjects actively converge focus on beads at different distances away along a string (Clark et al., 2015). Subjects are asked to adjust their fixation point to make sure two perceptual strings cross at the bead of fixation. In this paradigm, I saw differences in near versus far viewing in both binocularity measures and in amplitudes. This again indicates that fixation distance affects the behavior of microsaccades. The context of this study focused on binocularity and differences between near and far fixation conditions, but future studies with the Brock string or similar rehabilitation-focused paradigms may give greater insight into how active vision therapies improve and train eye coordination. Specifically, microsaccade binocularity, as well as amplitudes and rates can be compared before and after practicing with the Brock string to investigate whether microsaccades have a role in improving binocular coordination and convergence. A point of interest in assessing eye movements during the Brock string exercises is the active maintenance of vergence, as can be seen in the example eye traces in Figure 2.13 where the left and right eye slowly alternate in converging and verging on the brock bead target.

In comparison to the 3D spheres of the convergence board, microsaccade amplitudes during fixation of the far 3D spheres tended to be higher than during fixation of near, while the opposite is true in the Brock string exercise, with higher amplitudes during near fixation than far. I hypothesize that the size of the target on the retina may influence this difference in amplitude distributions of

near and far, as the near and far 3D spherical targets were molded to take up the same size on the retina, while the Brock string beads were not.

### 2.5.5 Binocularity Distributions in Microsaccades

The results summarized above show that the degree of disconjugacy of microsaccades, or their binocularity, can be affected by visual depth cues, as differences were found between binocularity distributions in near versus far viewing of spheres in 3D. In the literature discussing binocularity in microsaccades, there have been debates over whether disconjugate or monocular microsaccades are real. Some report a lack of detection of monocular microsaccades (Fang et al., 2018) and/or believe disconjugate microsaccades to be mislabeled or invalid detections from standard microsaccade detection algorithms (Nyström et al., 2017). However, disconjugate microsaccades and their characteristics have been recorded and studied in monkeys (Van Horn & Cullen, 2011) as well as in humans (Gautier et al., 2016), and there is a physiological basis to the presence of disconjugate microsaccades (see section 1.10). Furthermore, studies such as Nyström et al., 2017 used a 2D fixational cross as a target, which would not have provided any cues about depth to the visual system. Fang et al., 2018 did use small LEDs as fixation targets between 50-60cm from the subject and found very few monocular microsaccades. However, their study included paradigms with free head movements, which could have changed the characteristics of the microsaccades, and recorded eye movements using a Dual Purkinje Image eye tracker rather than a search coil, which may have failed to detect a subset of microsaccades.

### 2.5.6 Future Work

More studies and trials will be needed to fully understand how the degree of disconjugacy in microsaccades might change with depth cues. In this study, I found differences in binocularity and amplitude distributions between near and far fixational targets during both 3D viewing conditions as well as depth illusion conditions. Future work could look deeper into the properties of microsaccades in regards to illusional fixation. For example, Troncoso et al., 2008 and Otero-Millan et al., 2012 found that microsaccades drive illusory motion in the Enigma illusion and the rotating snakes illusion, suggesting possible roles for microsaccades in depth related illusions as well.

Lastly, the VOG system developed in this study was found to adequately approximate the coil trace, but had much greater noise in comparison to the eye coils. Therefore, some differences in microsaccade characteristics found in the eye coil data were missed using the VOG system, emphasizing the need for minimal noise in microsaccade characterization. With adjustments to factors such as lighting, zoom, or head mobility, the VOG system has the potential to reduce noise and more accurately record microsaccades. This could allow for less reliance on the eye coils and their inherent invasive requirements.

# Chapter 3: DISCUSSION

## 3.1 Summary

In this thesis, I measured microsaccades during fixation of various 2D and 3D targets and examined characteristics of binocularity, amplitude, main sequence slopes, and rate. I found microsaccade binocularity, amplitudes, and main sequence slopes to be significantly different between the near and far conditions of the 3D convergence board, Brock string bead exercise, and the depth illusion paradigms. I also found microsaccade amplitude distributions often differed between paradigms, with the Magic Eye amplitudes especially high. Thus, my data suggests that depth cues produce differences in perception processing, leading to differences in microsaccade behavior.

## 3.2 The VOG System

During my experiments, I recorded eye movements using an eye coil system concurrently with our developed VOG system to validate whether the VOG system could record accurately enough to warrant future use without eye coils. In particular, I wanted to confirm whether my main findings obtained using eye coils could also be demonstrated using our VOG system.

Overall, my analysis of the VOG data resulted in similar conclusions to my analysis of the eye coil data. Notably, when comparing distributions of binocularity between near and far, both coil and VOG data showed significant differences between some of the same paradigms, namely the 3D sphere targets, the spiral depth illusion, and the Brock string exercise. Comparing amplitude distributions also produced similar results between the coil and VOG system, though with some discrepancies in directional bias of microsaccade amplitudes and in the degree of

significant difference. Furthermore, the average variance accounted for (VAF) between sampled eye coil and VOG traces was calculated to be .86±.15, suggesting that the VOG system can approximate coil results to a certain extent.

However, despite the similarities found between eye coil and VOG results, the VOG recordings contained noise levels that were 90% higher than in the former. These higher noise levels limit the ability to quantify microsaccade characteristics, as seen by how the eye coils recorded differences in characteristics that did not reach significance in the VOG data. Thus, accurate characterization of microsaccades requires the use of eye recording techniques with minimal noise. VOG recordings showed both low and high frequency noise (Figure 2.5D), the low frequency noise possibly due to head movements as the bite bar is quite limited in restricting head movements, and the high frequency noise likely due to algorithmic noise inherent to our pupil tracking approach. Eye coil noise was minimal and may be due to the conversion of the signals from analog to digital.

Given that there was on average 90% less noise in the eye coil than in the VOG traces, I focused my analysis and discussion in chapter 2 on the data from eye coil recordings. Other studies have compared different VOG systems with eye coils as well. For example, van der Geest & Frens, 2001 compared the EyeLink version 2.04 with the eye coil technique on recording fixations and saccades and found saccade parameters of amplitude, duration and peak velocities were highly correlated between the two systems, but that the video system's low frame rate of 250Hz compared to the eye coil's 500Hz limited the accuracy of the saccade peak velocities. In another study, Houben, Goumans & van der Steen, 2006 compared the Chronos, a video-based infrared 3D eye tracker with a 200Hz frame rate, with the coil method at 1000Hz sampling during fixation, saccades, and optokinetic and vestibular stimulation, and found

saccade parameters of peak velocity and duration to be correlated but not completely identical. Both van der Geest & Frens, 2001 and Houben, Goumans & van der Steen, 2006 concluded that coils provide better signals, but that these early VOGs could be good alternatives for less demanding tests. Lastly, in a more recent study, McCamy et al., 2015 simultaneously recorded microsaccades using an EyeLink 1000 video system sampled at 1000Hz with a coil system also at 1000Hz and found that 95% of microsaccades detected with each system to be also detected in the other. Notably, all these studies found that peak velocities and main sequence slopes were higher in VOG tracking compared to eye coil tracking.

Indeed, with continual improvements in the camera systems and tracking algorithms, I speculate that we will see further improvements in VOG systems such that noise levels become low enough to allow for highly accurate non-invasive eye tracking of microsaccades in humans. Future studies could also consider tracking head movement to test if removing such signals produces cleaner VOG data.

### 3.3 Future work

As the ranges for the microsaccade rates across paradigms and depth viewing are quite large, I do not dismiss the possibility of microsaccades being missed or mislabeled by the algorithm used. This thesis project used an adaption of the microsaccade detection algorithm developed by Engbert & Kliegl, as this algorithm has been commonly used in the literature. This algorithm, however, is about 20 years old now, and while it generally detects microsaccades well, it may not be the most accurate algorithm possible. Recent studies have looked into different methods for microsaccade detection; for example, Otero-Millan et al., 2014 found that an unsupervised clustering method gave 62% fewer errors for binocular data, and 78% fewer for

monocular data, compared to the Engbert & Kliegl algorithm. In future work, perhaps a new microsaccade detection strategy such as this unsupervised clustering method could be used.

This study also did not characterize microsaccades during the Brock string exercise over time or examine improvement in convergence. However, this may be an important area for the study of eye movements in vision therapies. Future work might be able to look at microsaccades during free viewing of targets at different depths, or go into greater depth of analysis on their role in vision therapies such as the Brock string exercise, which requires longer fixational gazes on each bead and additional practice times.

### 3.4 Conclusion

In conclusion, while microsaccades are mostly conjugate, the presence of disconjugate microsaccades should not be discounted. Our results may give new insight into how microsaccades are influenced by depth cues, and how the processing of bottom-up feedback may affect eye movements.

# TABLES

| Eye movement | | Function |
|---|---|---|
| **Saccades** | Voluntary | Redirecting gaze |
| **Smooth pursuit** | Voluntary | Tracking moving objects |
| **Vergence** | Voluntary | Rotating eyes to look at different depths |
| **Vestibulo-ocular reflex** | Involuntary | Keeping retinal images stable while the head moves |
| **Optokinetic reflex** | Involuntary | Stabilizing vision during movement of peripheral targets |

**Table 1.1:** Classes of eye movements. Microsaccades fall under the category of saccades, but are involuntary movements.

| | Coil near | Coil far | F test value | Significant difference |
|---|---|---|---|---|
| **3Dboard** | 30.31 | 25.28 | 38.97 | 1 |
| **2Dboard** | 25.95 | 24.59 | 5.96 | 1 |
| **Magic Eye** | 24.14 | 24.89 | 3.07 | 0 |
| **Spiral Illusion** | 27.59 | 30.08 | 25.41 | 1 |
| **Brock String** | 23.84 | 26.37 | 7.13 | 1 |

**Table 2.1:** Main sequence slopes over all subjects for each condition, including F-test values between near and far slopes and resulting significant difference. 1 signifies that the F-test value conveys a significant difference; Differences were found in slopes between near and far fixation main sequence for all paradigms except the Magic Eye.

| | Near fixation | Near stdev | Far fixation | Far stdev |
|---|---|---|---|---|
| **3Dboard** | 1.36 | 0.28 | 1.56 | 0.66 |
| **2Dboard** | 1.15 | 0.48 | 1.25 | 0.56 |
| **Magic Eye** | 1.13 | 0.25 | 1.17 | 0.66 |
| **Spiral Illusion** | 1.23 | 0.39 | 1.32 | 0.45 |
| **Brock string** | 1.34 | 0.62 | 1.33 | 0.61 |

**Table 2.2:** Average microsaccade rates for each paradigm, in microsaccades per second. No significant differences were found between near and far microsaccade rates.

| | 2D vs 3D: Near BI | 2D vs 3D Far BI | 2D vs 3D : Near Amp | 2D vs 3D: Far Amp |
|---|---|---|---|---|
| **Coil recordings** | .0004*** | .8814 | <.0001*** | <.0001*** |
| **VOG recordings** | .0825 | .2658 | .0197* | <.0001*** |

**Table 2.3:** Summarizing significant differences between binocularity and amplitude distributions during 2D vs 3D fixation of the convergence board targets, determined by p-values given by nonparametric 2-tailed t-tests. A p-value under .05 signifies rejection of the null hypothesis.
The number of *'s next to a p-value indicates the level of significance, where $p < .05$ = *, $p < .01$ = **, and $p < .001$ = ***. Purple stars represent if the 3D condition has a greater level of disconjugacy or a greater median amplitude; Yellow stars represent the same but for the 2D condition. Coil recordings of microsaccades show great significant differences between 2D and 3D sphere fixation conditions where the 3D condition gave greater proportions of disconjugate microsaccades. There appears to be some match between the eye coil and VOG systems in amplitude related significant findings.

| Characteristic | Binocularity Index | | Amplitude | |
|---|---|---|---|---|
| Comparison | Coil: Near vs far | VOG: near vs far | Coil: Near vs far | VOG: near vs far |
| **3Dboard** | <.0001*** | .0001*** | .0299* | <.0001*** |
| **2Dboard** | .1798 | .7248 | .5067 | .1524 |
| **Magic Eye** | .6082 | .0553 | .2634 | .0213* |
| **Spiral Illusion** | <.0001*** | .8071 | .0016** | .3198 |
| **Brock string** | .0001*** | .0125** | <.0001*** | <.0001*** |

**Table 2.4:** Significant differences between disconjugacy and amplitude distributions, determined by p-values given by nonparametric 2-tailed t-test comparisons. A p-value under .05 signifies rejection of the null hypothesis. Binocularity, or disconjugacy distributions, are quantified by the binocularity index measured for each microsaccade.
The number of *'s next to a p-value indicates the level of significance, where $p < .05$ = *, $p < .01$ = **, and $p < .001$ = ***. Green stars represent if the near condition has a greater level of disconjugacy or a greater median amplitude; Red stars represent the same but for the far condition. Significant differences were found consistently across both binocularity and amplitude distributions for the 3D sphere board, spiral depth illusion, and Brock string exercises.

# FIGURES

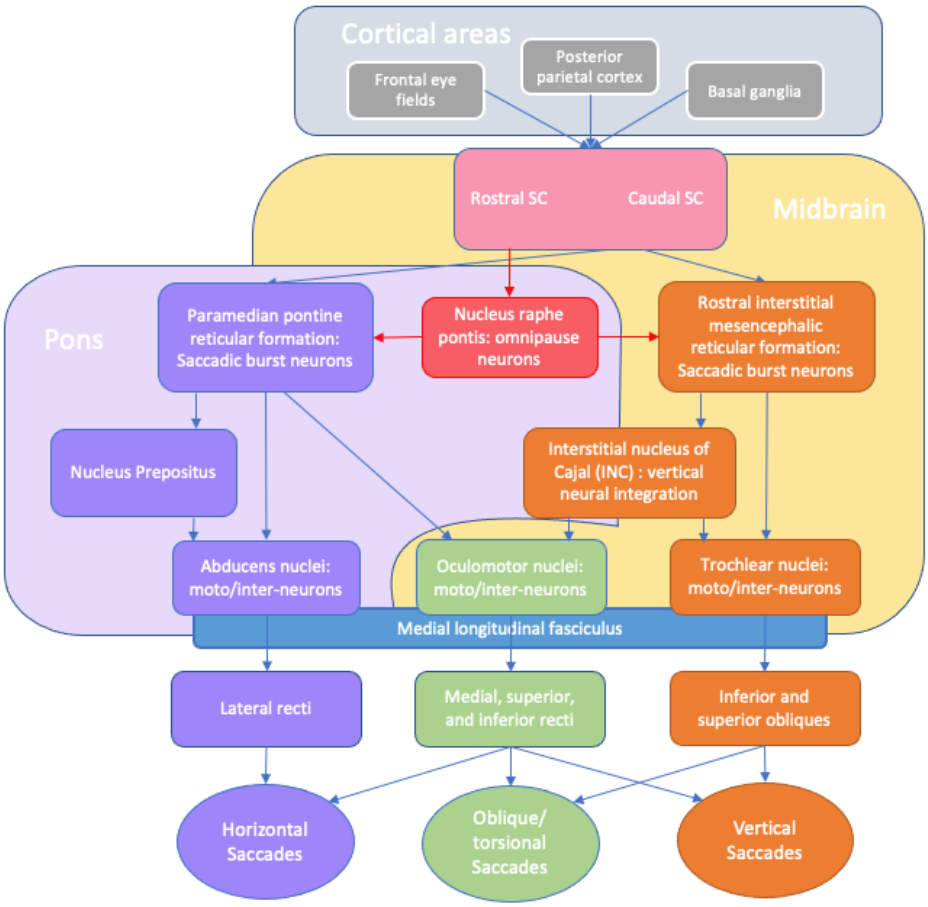


**Figure 1.1:** The saccadic pathway. The superior colliculus (SC) receives input from various cortical areas, and is organized as a gaze control motor map. Stimulation towards the caudal side of the SC drives higher amplitude saccades, and stimulation away from the midline (which runs from the rostral to caudal ends) drives larger changes in saccade direction. Microsaccades are generated in the rostral side of the SC, which also projects to the nucleus raphe pontis (NRP). The NRP holds omnipause neurons that pause in firing during saccadic movements. Generation of saccades is found in two main parallel pathways that run generally through the midbrain for vertical saccades and through the pons for horizontal saccades. Saccadic burst neurons (SBNs) both in the pons and the midbrain project to a nuclei layer, from which the medial longitudinal fasciculus (MLF) helps coordinate the eye muscles such that conjugate movements are produced with the two eyes.

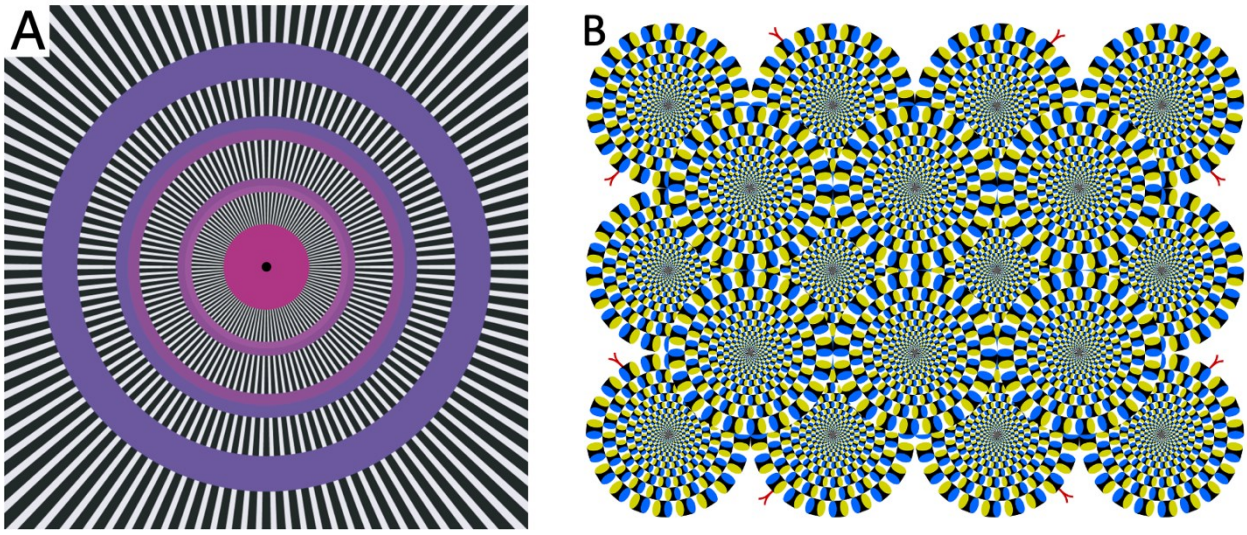


**Figure 1.2:** A). The Enigma illusion (Troncoso et al., 2007). B). The rotating snakes illusion (Otero-Millan et al., 2012).

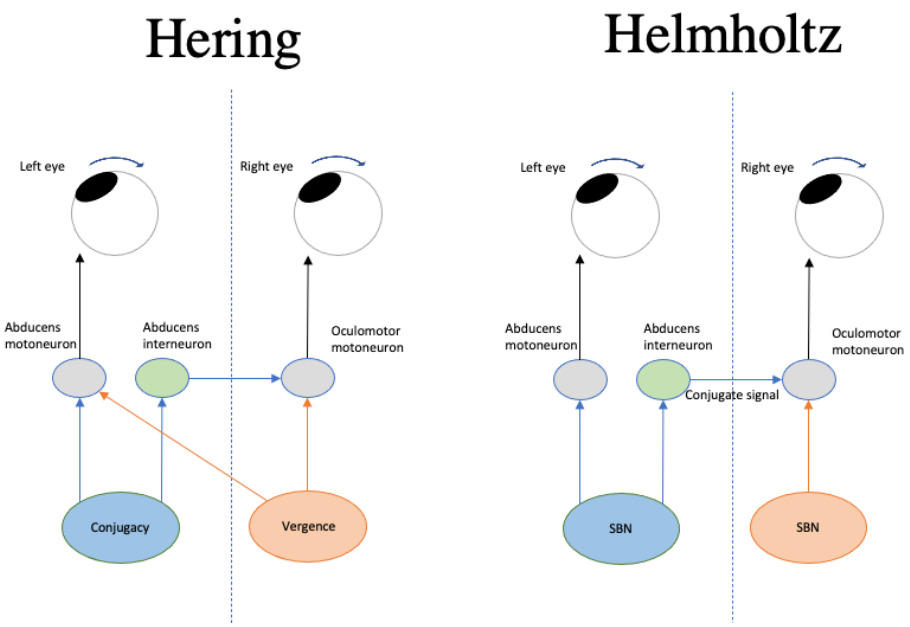


**Figure 1.3:** The neural control of disconjugate saccades. Ewald Hering believed that the eye muscles were equally innervated, resulting in primarily conjugate eye movements. Following Hering's 'law of equal innervation', microsaccades have classically thought to be conjugate movements, modified by outside vergence commands. On the other side of the Binocular Control debate was Hermann von Helmholtz, who believed the eyes to be initially wired to move independently. Saccades have now been shown to be encoded by saccadic burst neurons (SBNs) for each individual eye, disproving Hering's law and providing a neural basis for disconjugate eye movements.

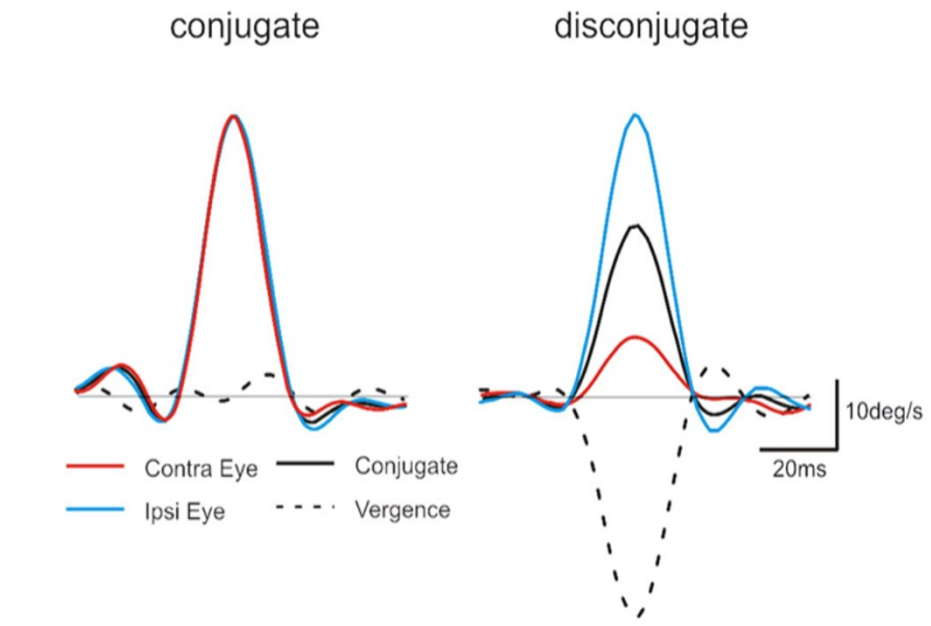


**Figure 1.4:** Example velocity traces for conjugate and disconjugate microsaccades. (Van Horn & Cullen, 2011)

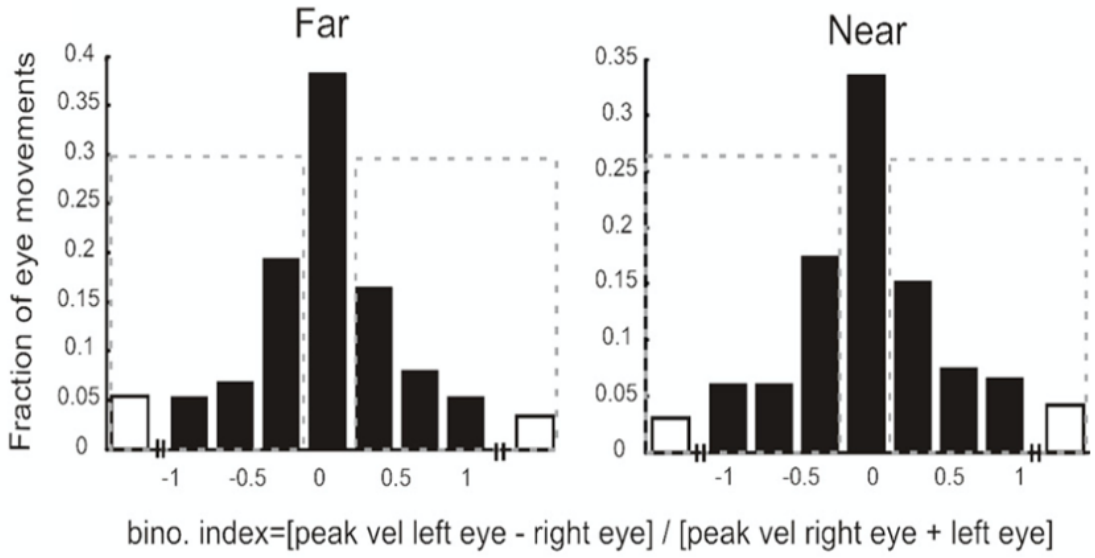


**Figure 1.5:** Distribution of binocularity or the degree of conjugacy for microsaccades found during far and near viewing in non-human primates (Van Horn & Cullen, 2011). White squares indicate fully monocular movements.

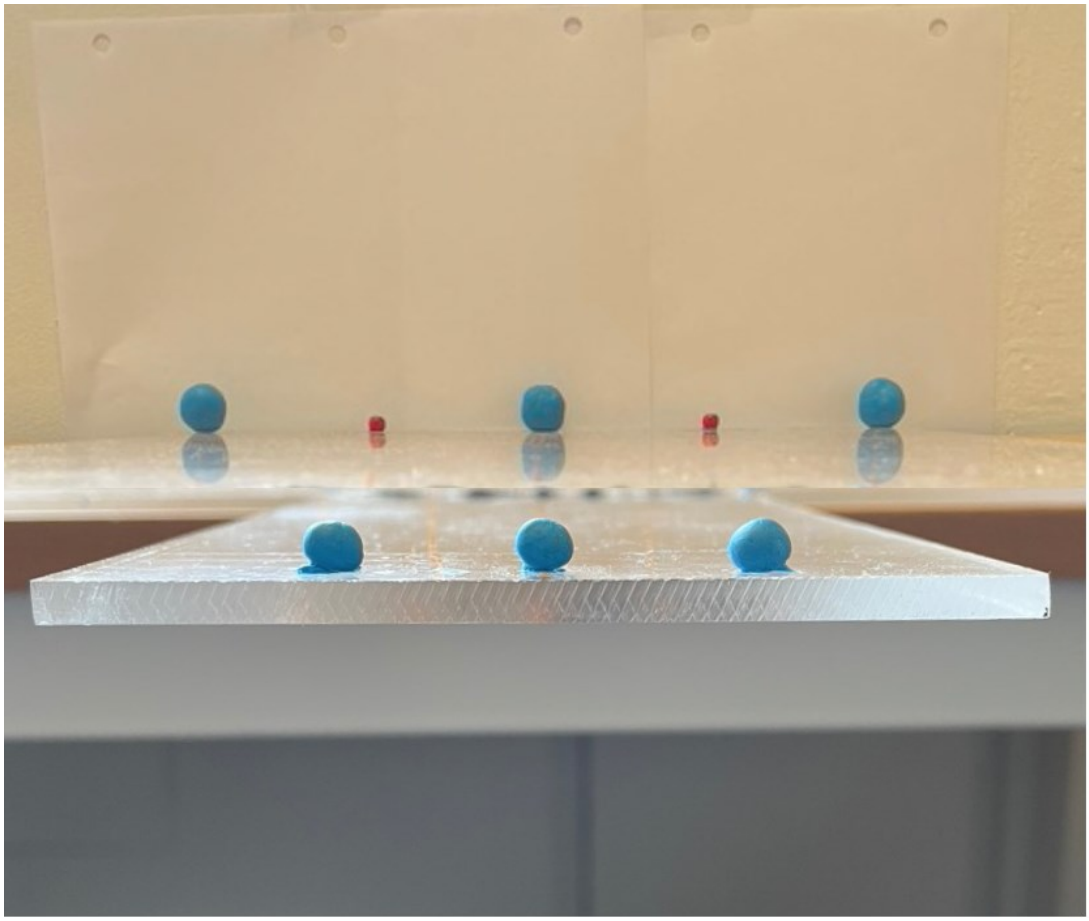

**Figure 2.1:** 2D control image of 3D convergence board spheres

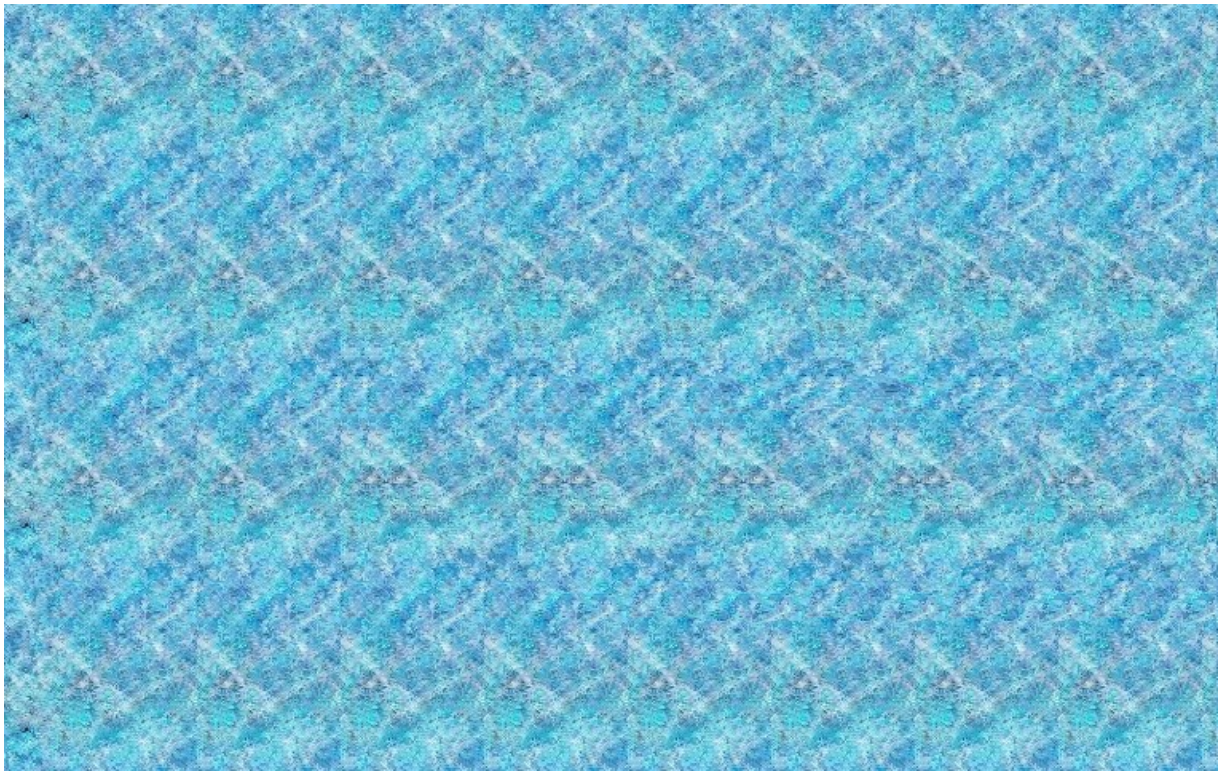

**Figure 2.2:** Magic Eye image. Seeing the hidden 3D donut requires convergence of the eyes. Subjects moved between discrete points within near or far areas of the donut.

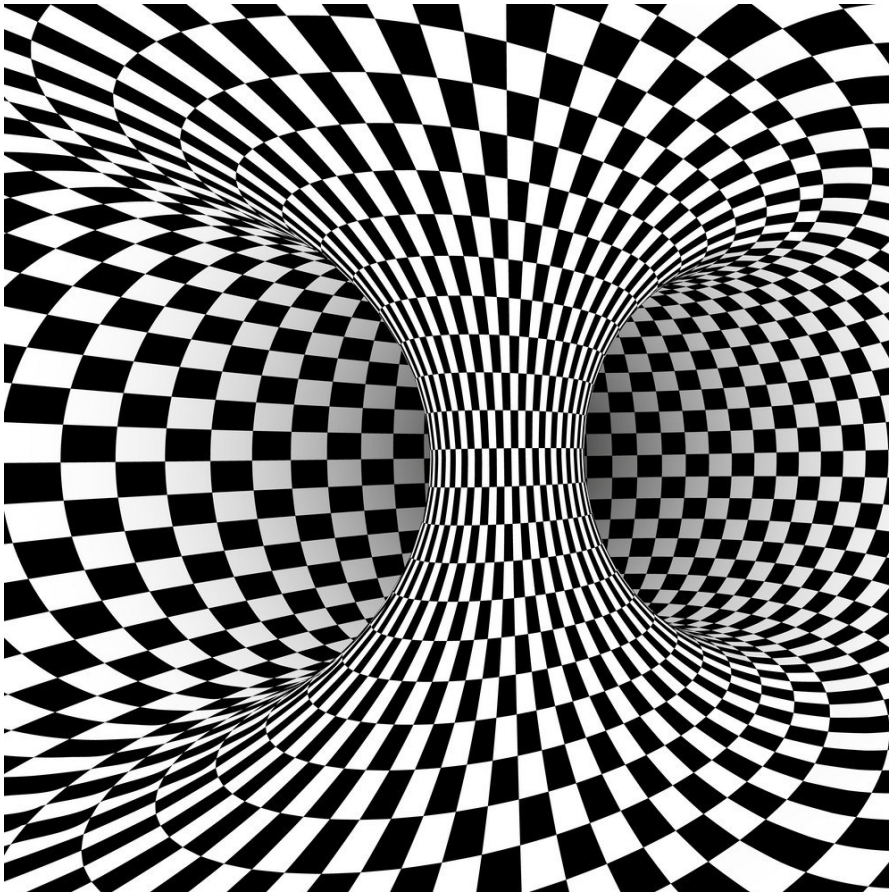

**Figure 2.3:** The spiral depth illusion. Subjects alternated fixating on spots in near and far looking areas.

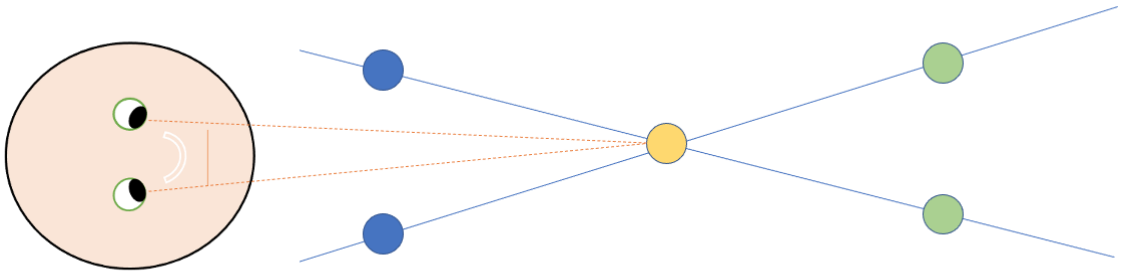

**Figure 2.4:** An example of how the Brock string exercise works. When looking at the middle bead, the subject should see 2 strings and sets of near and far beads, and the strings should cross at the bead. Seeing the strings cross before or after the bead requires adjusting one's gaze such that the strings cross in or at the bead. This exercise helps the eyes practice fixating binocularly, with equal coordination.

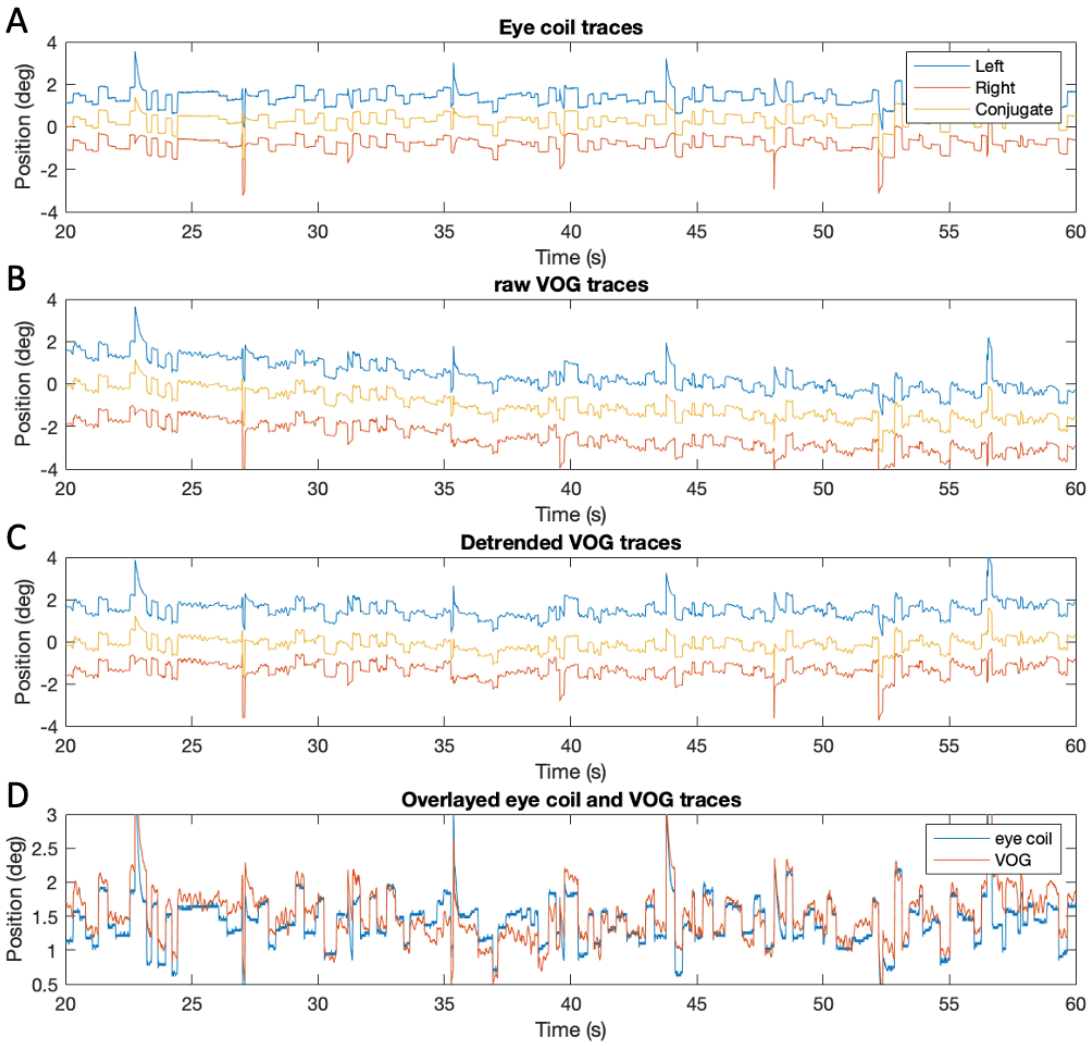


**Figure 2.5:** Example traces during convergence board target fixation from the same example subject and recording time. Both eyes were recorded simultaneously using the VOG and eye coil systems, with left, right, and conjugate position traces shown. A). Eye coil traces. B). Raw VOG traces. C). Detrended VOG traces. D). Overlayed eye coil and VOG traces. The VOG eye position trace has larger noise oscillations and carries some drift compared to the eye coil position trace, but overall follows the eye coil fairly well. Further analysis mostly focused on data generated by the eye coils.

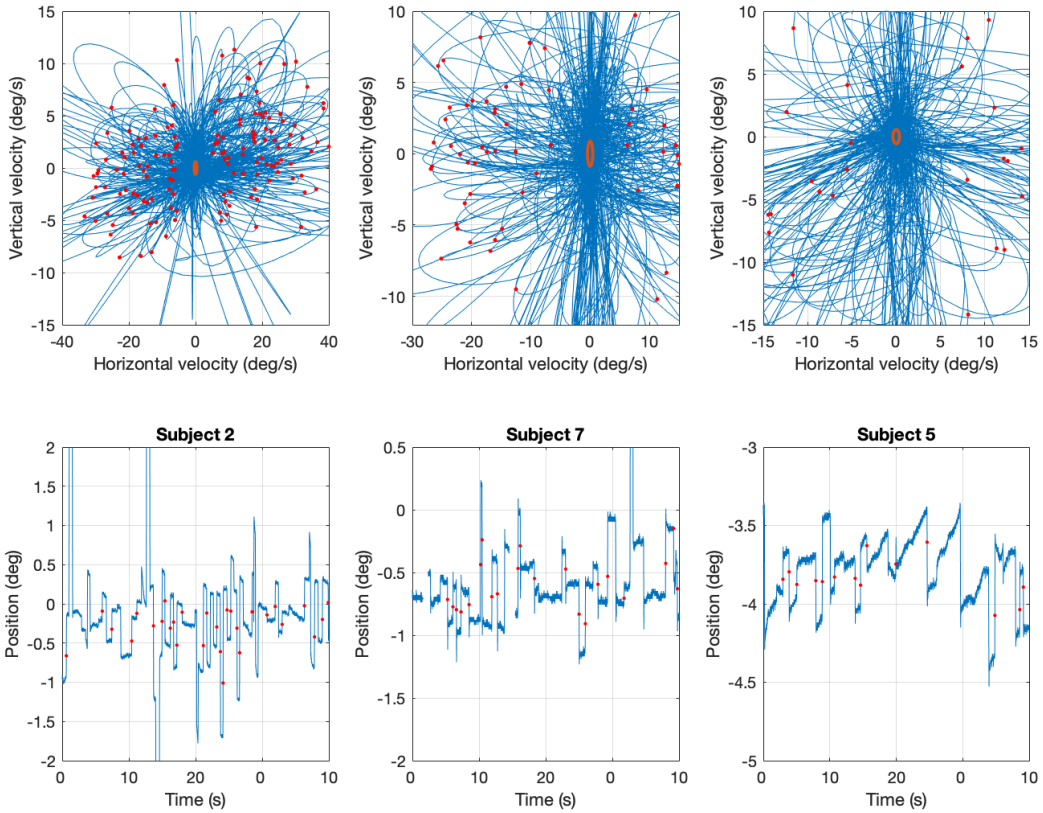


**Figure 2.6:** Three examples of microsaccade detection. The top figures are examples of how the microsaccade detection algorithm works. Velocity points outside an elliptical threshold boundary are then separated into individual microsaccades. Red dots indicate position of peak velocity for each microsaccade.

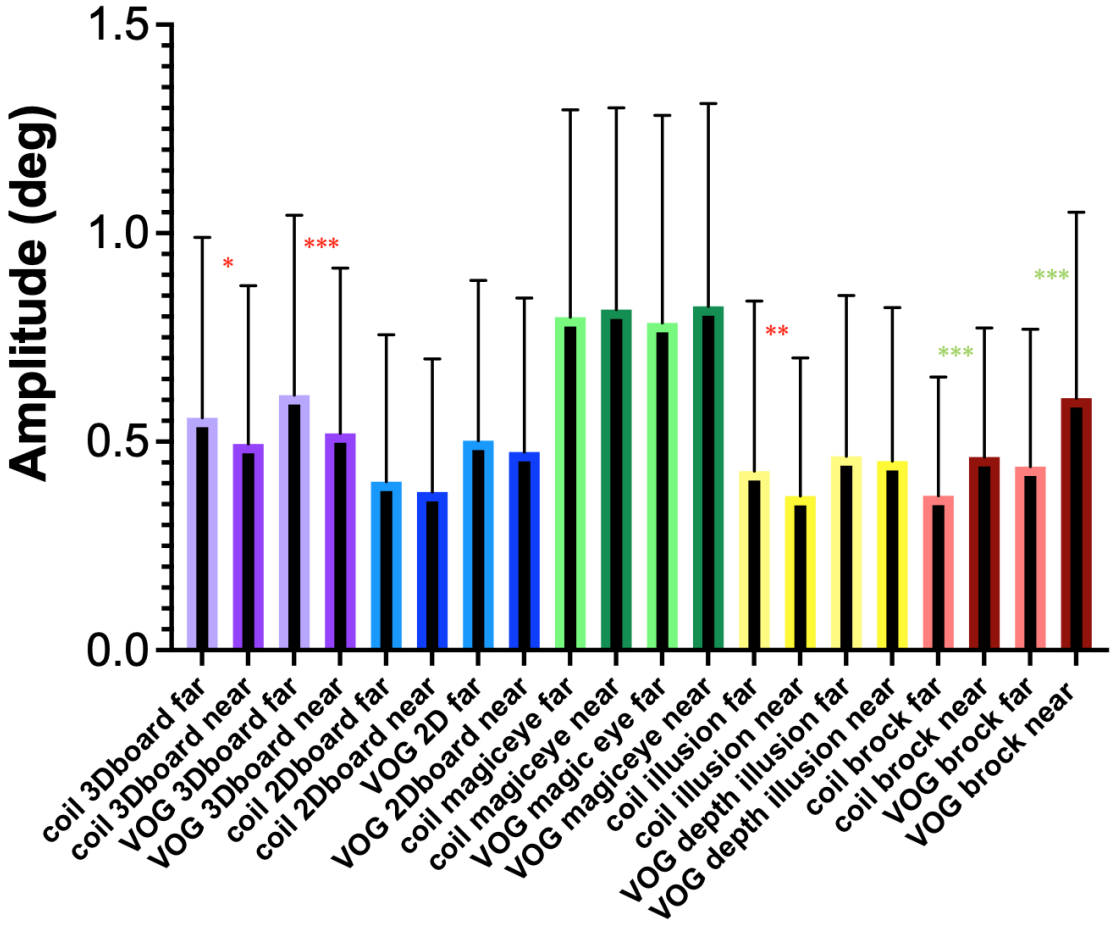


**Figure 2.7:** Mean amplitudes of microsaccades for each condition and paradigm with standard deviations. P-values for near and far conditions of each paradigm are listed in Table 2.4. Similar to Table 2.4, the number of *'s between a pair of near and far condition bars symbolizes the level of significance, where $p < .05$ = *, $p < .01$ = **, and $p < .001$ = ***. Green stars represent if the near condition has a greater level of disconjugacy or a greater median amplitude; Red stars represent the same but for the far condition. Significant differences were found consistently across both binocularity and amplitude distributions for the 3D sphere board, spiral depth illusion, and Brock string exercises.

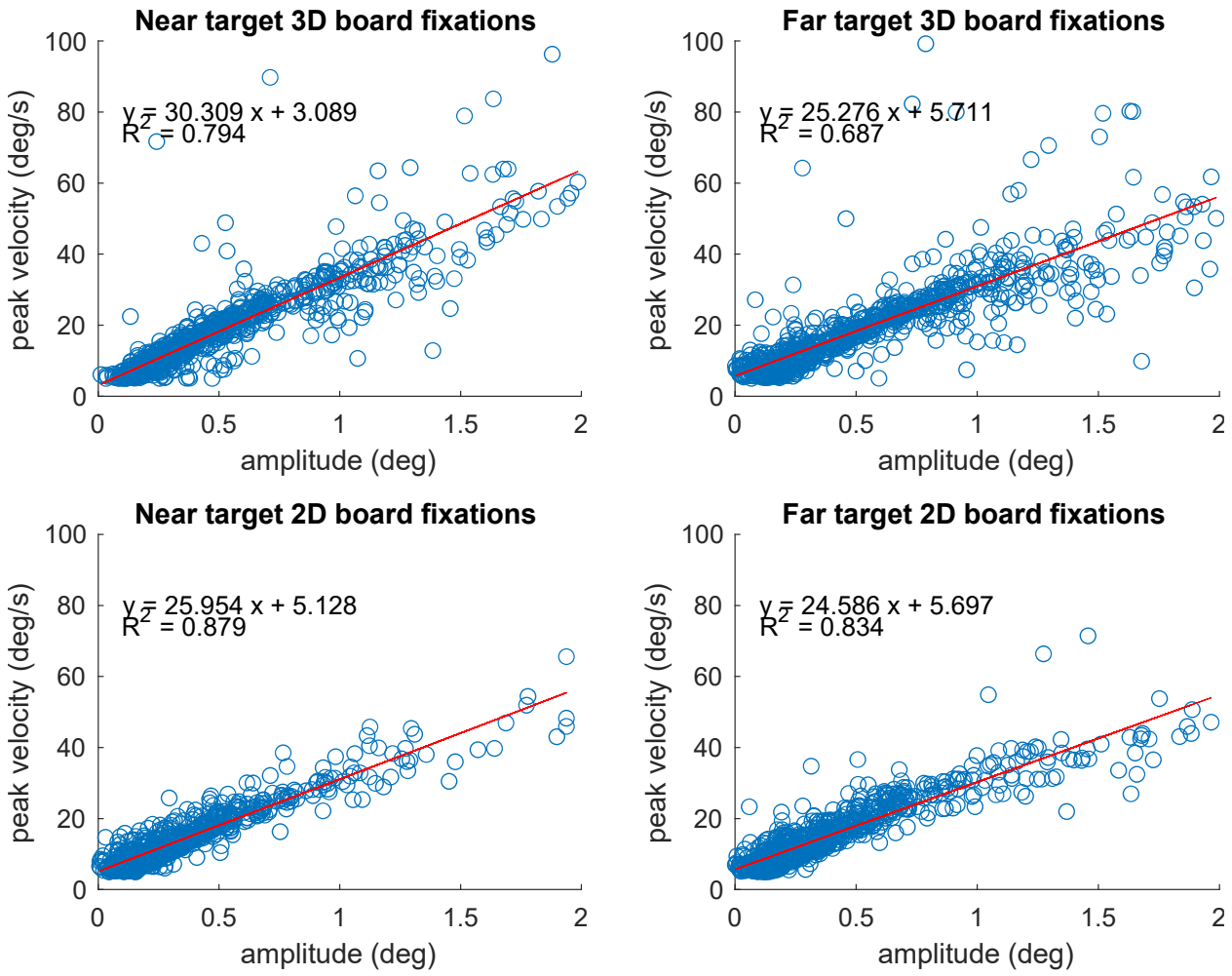


**Figure 2.8:** Main sequences of microsaccades from near and far fixation of 3D and 2D spheres, main sequences from the Magic Eye, Spiral illusion, and Brock String paradigms not shown. Slopes can be found in Table 2.1, data analysis used eye coil traces. Microsaccades show linear trends when plotting peak velocity against amplitude, consistent with previous studies. Significant differences were found between near and far main sequence slopes for all paradigms except the Magic Eye paradigm.

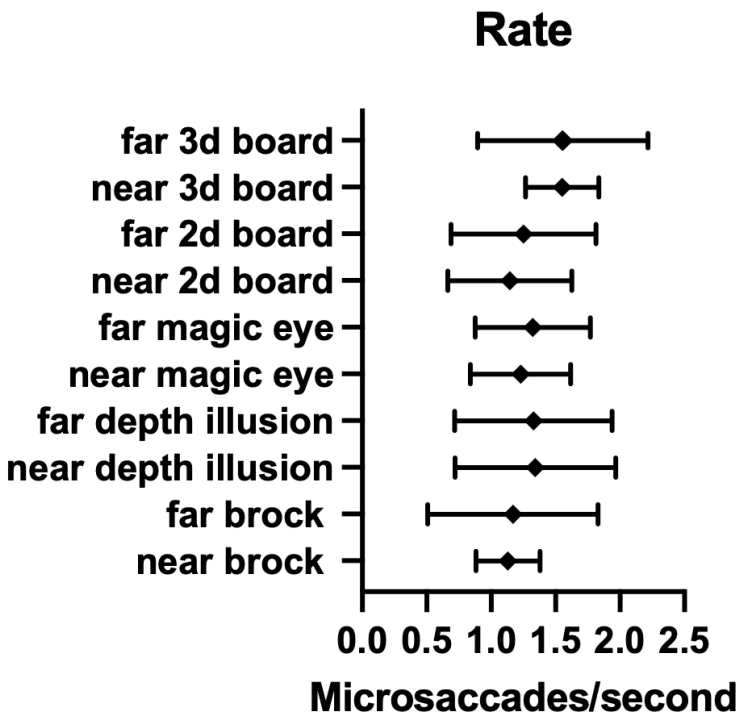


**Figure 2.9:** Average microsaccade rates for each paradigm indicated by diamonds, in microsaccades per second. Error lines indicate standard deviation. Rates were not found to have any significant differences between conditions.

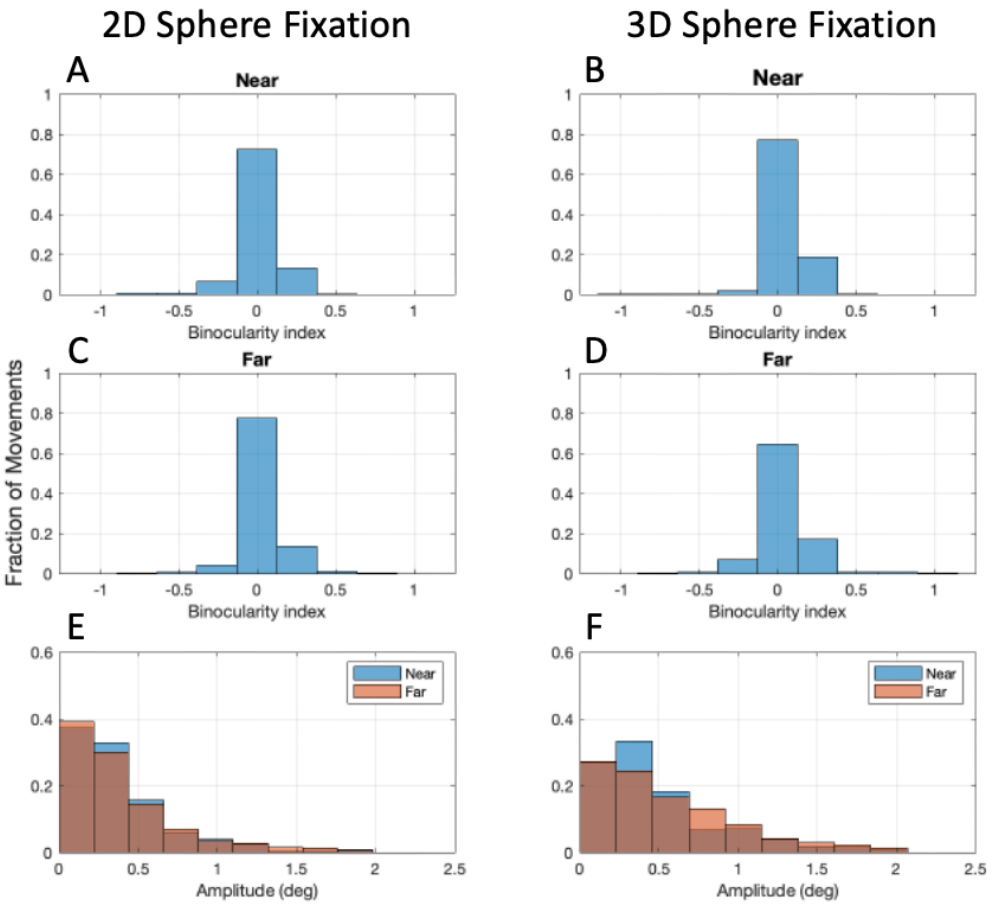


**Figure 2.10:** Microsaccade characteristics during 2D vs 3D sphere fixations. A-D): Binocularity distributions during fixation of the A). Near 2D sphere, B). Near 3D sphere, C). Far 2D sphere, and D). Far 3D sphere. E). Amplitude distribution of microsaccades during near and far 2D sphere fixations. F). Amplitude distribution of microsaccades during near and far 3D sphere fixations.
In comparing microsaccade characteristics between 2D vs 3D spheres for both near and far conditions,, significant differences were found between the 2D and 3D fixations of near binocularity and near and far amplitude distributions. In comparing between near and far conditions for the 2D, no significant differences were found in both binocularity and amplitude distributions. In the 3D sphere paradigm, binocularity of microsaccades between the near and far conditions were found to be significantly different, and microsaccades during far sphere fixation seem to have a greater fraction of disconjugate movements, as indicated by its lower proportion of fully conjugate movements. P-values for comparisons are recorded in Table 2.4.

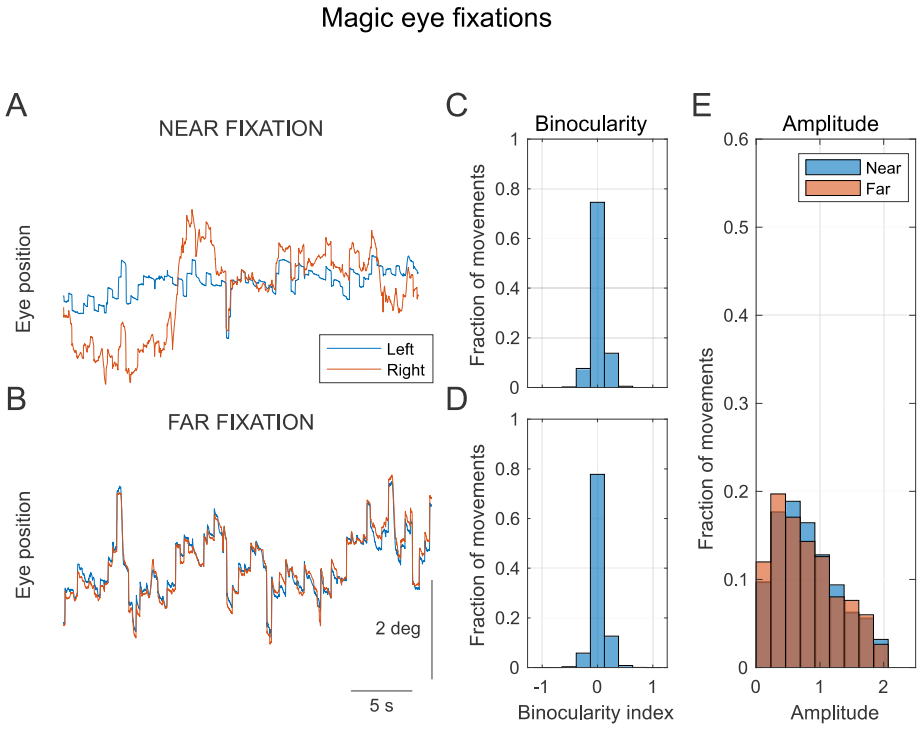


**Figure 2.11:** Example traces, binocularity distributions, and amplitude distributions for microsaccades in near and far fixation during the Magic Eye task. A). Example eye coil traces during near fixation for left and right eye movements. B). Example eye coil traces during far fixation for left and right eye movements. C). Binocularity distribution for microsaccades derived from the eye coil trace during near fixation. D). Binocularity distribution for microsaccades derived from the eye coil trace during far fixation. E). Amplitude distributions based on microsaccades derived from the eye coil traces for both near and far fixation.

Binocularity and amplitude histograms are graphed with data from all subjects combined. A and B show examples of how eye positions between the right and left move in disconjugate and disconjugate movements respectively. Graphs in the top row show data from near fixation, the bottom row showing data from far fixation. Microsaccades between near and far fixation during the Magic Eye task were not found to be significantly different in both binocularity and amplitude distributions.

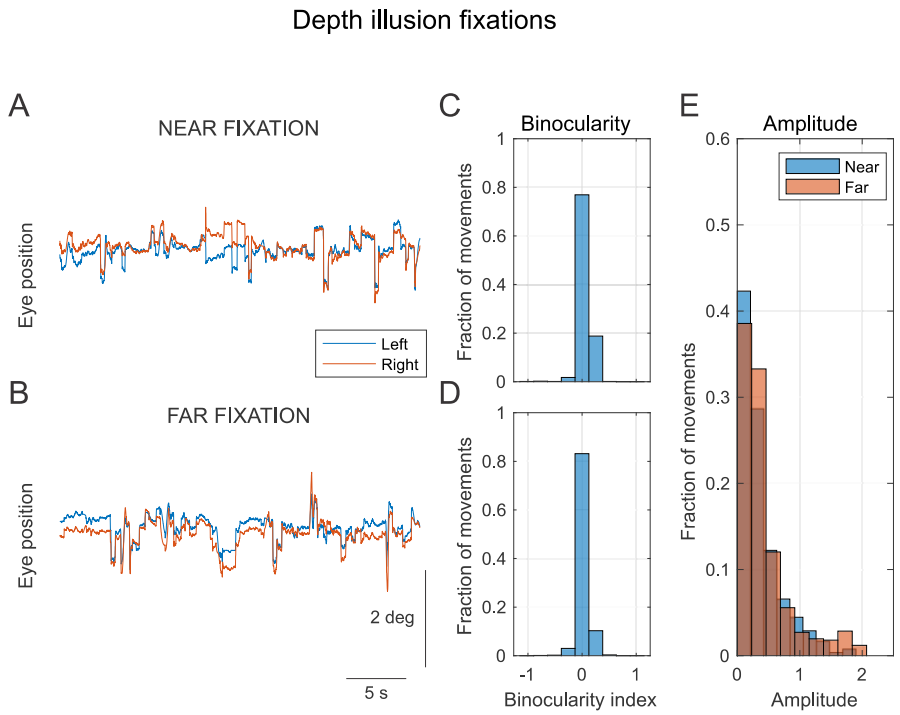


**Figure 2.12:** Example traces, binocularity distributions, and amplitude distributions for microsaccades in near and far fixation during the spiral depth illusion exercise. Binocularity and amplitude histograms are graphed with data from all subjects combined. Binocularity and amplitude distributions were significantly different between microsaccades during near and far fixation. In graphs C vs D, the binocularity of microsaccades during near fixation seem to have higher proportions of disconjugate microsaccades, while graph E indicates that the far fixation microsaccades tend to be larger in amplitude.

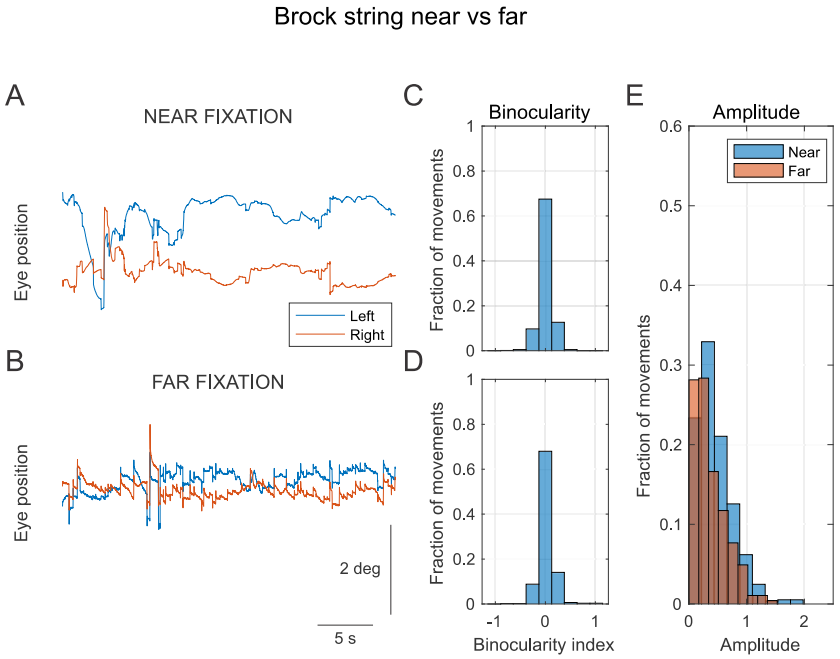


**Figure 2.13**: Example traces, binocularity distributions, and amplitude distributions for microsaccades in near and far fixation during the Brock string exercise task. A and B). Active convergence and vergence movements can be seen in the eye movements traces as the subject adjusts their gaze on the brock string beads. C and D). Significant differences were found between binocularity of near vs far fixation during the Brock String exercise. Microsaccades during far fixation seem to have a greater difference in proportions of disconjugate movements made by the left and right eye, compared to during near fixation in which these proportions are more similar. E). Amplitudes between near and far fixation form separate, significantly different distributions, with the near fixational microsaccades having generally higher amplitudes.

## REFERENCES


Bridgeman, B., & Palca, J. (1980). The role of microsaccades in high acuity observational tasks. *Vision Research*, *20*(9), 813–817. https://doi.org/10.1016/0042-6989(80)90013-9

Clark, J. F., Colosimo, A., Ellis, J. K., Mangine, R., Bixenmann, B., Hasselfeld, K., Graman, P., Elgendy, H., Myer, G., & Divine, J. (2015). Vision training methods for sports concussion mitigation and management. *Journal of Visualized Experiments: JoVE*, *99*, e52648. https://doi.org/10.3791/52648

Cullen, K. E., & Guitton, D. (1997). Analysis of Primate IBN Spike Trains Using System Identification Techniques. II. Relationship to Gaze, Eye, and Head Movement Dynamics During Head-Free Gaze Shifts. *Journal of Neurophysiology*, *78*(6), 3283–3306. https://doi.org/10.1152/jn.1997.78.6.3283

Dodge, R. (1903). Five types of eye movement in the horizontal meridian plane of the field of regard. *American Journal of Physiology-Legacy Content*, *8*(4), 307–329. https://doi.org/10.1152/ajplegacy.1903.8.4.307

Engbert, R., & Kliegl, R. (2003). Microsaccades uncover the orientation of covert attention. *Vision Research*, *43*(9), 1035–1045. https://doi.org/10.1016/S0042-6989(03)00084-1

Engbert, R., & Kliegl, R. (2004). Microsaccades Keep the Eyes' Balance During Fixation. *Psychological Science*, *15*(6), 431–431. https://doi.org/10.1111/j.0956-7976.2004.00697.x

Fang, Y., Gill, C., Poletti, M., & Rucci, M. (2018). Monocular microsaccades: Do they really occur? *Journal of Vision*, *18*(3), 18–18. https://doi.org/10.1167/18.3.18

Gautier, J., Bedell, H. E., Siderov, J., & Waugh, S. J. (2016). Monocular microsaccades are visual-task related. *Journal of Vision*, *16*(3), 37–37. https://doi.org/10.1167/16.3.37

Hafed, Z. M., & Clark, J. J. (2002). Microsaccades as an overt measure of covert attention shifts. *Vision Research*, *42*(22), 2533–2545. https://doi.org/10.1016/S0042-6989(02)00263-8

Hafed, Z. M., Goffart, L., & Krauzlis, R. J. (2009). A neural mechanism for microsaccade generation in the primate superior colliculus. *Science (New York, N.Y.)*, *323*(5916), 940–943. https://doi.org/10.1126/science.1166112

Harrison, J. J., Sumner, P., Dunn, M. J., Erichsen, J. T., & Freeman, T. C. A. (2015). Quick Phases of Infantile Nystagmus Show the Saccadic Inhibition Effect. *Investigative Ophthalmology & Visual Science*, *56*(3), 1594–1600. https://doi.org/10.1167/iovs.14-15655

Horn, M. R. V., Mitchell, D. E., Massot, C., & Cullen, K. E. (n.d.). *Local Neural Processing and the Generation of Dynamic Motor Commands within the Saccadic Premotor Network*. 13.

Houben, M. M. J., Goumans, J., & Steen, J. van der. (2006). Recording Three-Dimensional Eye Movements: Scleral Search Coils versus Video Oculography. *Investigative Ophthalmology & Visual Science*, *47*(1), 179–187. https://doi.org/10.1167/iovs.05-0234

Jang, J. U., Jang, J. Y., Tai-hyung, K., & Moon, H. W. (2017). Effectiveness of Vision Therapy in School Children with Symptomatic Convergence Insufficiency. *Journal of Ophthalmic & Vision Research*, *12*(2), 187–192. https://doi.org/10.4103/jovr.jovr_249_15

Judge, S. J., & Cumming, B. G. (1986). Neurons in the monkey midbrain with activity related to vergence eye movement and accommodation. *Journal of Neurophysiology*, *55*(5), 915–930. https://doi.org/10.1152/jn.1986.55.5.915

King, W. M. (2011). Binocular Coordination of Eye Movements: Hering's Law of Equal Innervation or Uniocular Control? *The European Journal of Neuroscience*, *33*(11), 2139–2146. https://doi.org/10.1111/j.1460-9568.2011.07695.x

Krauskopf, J., Cornsweet, T. N., & Riggs, L. A. (1960). Analysis of Eye Movements during Monocular and Binocular Fixation*. *JOSA*, *50*(6), 572–578. https://doi.org/10.1364/JOSA.50.000572

Luschei, E. S., & Fuchs, A. F. (1972). Activity of brain stem neurons during eye movements of alert monkeys. *Journal of Neurophysiology*, *35*(4), 445–461. https://doi.org/10.1152/jn.1972.35.4.445

Malinov, I. V., Epelboim, J., Herst, A. N., & Steinman, R. M. (2000). Characteristics of saccades and vergence in two kinds of sequential looking tasks. *Vision Research*, *40*(16), 2083–2090. https://doi.org/10.1016/S0042-6989(00)00063-8

Martinez-Conde, S., Macknik, S. L., Troncoso, X. G., & Hubel, D. H. (2009). Microsaccades: A neurophysiological analysis. *Trends in Neurosciences*, *32*(9), 463–475. https://doi.org/10.1016/j.tins.2009.05.006

Maxwell, J., Tong, J., & Schor, C. M. (2012). Short-term adaptation of accommodation, accommodative vergence and disparity vergence facility. *Vision Research*, *62*, 93–101. https://doi.org/10.1016/j.visres.2012.03.013

Mays, L. E. (1984). Neural control of vergence eye movements: Convergence and divergence neurons in midbrain. *Journal of Neurophysiology*, *51*(5), 1091–1108. https://doi.org/10.1152/jn.1984.51.5.1091

McCamy, M. B., Otero-Millan, J., Di Stasi, L. L., Macknik, S. L., & Martinez-Conde, S. (2014). Highly informative natural scene regions increase microsaccade production during visual scanning. *The Journal of Neuroscience: The Official Journal of the Society for Neuroscience*, *34*(8), 2956–2966. https://doi.org/10.1523/JNEUROSCI.4448-13.2014

McCamy, M. B., Otero-Millan, J., Leigh, R. J., King, S. A., Schneider, R. M., Macknik, S. L., & Martinez-Conde, S. (2015). Simultaneous Recordings of Human Microsaccades and Drifts with a Contemporary Video Eye Tracker and the Search Coil Technique. *PLOS ONE*, *10*(6), e0128428. https://doi.org/10.1371/journal.pone.0128428

Møller, F., Laursen, M., Tygesen, J., & Sjølie, A. (2002). Binocular quantification and characterization of microsaccades. *Graefe's Archive for Clinical and Experimental Ophthalmology*, *240*(9), 765–770. https://doi.org/10.1007/s00417-002-0519-2

Nyström, M., Andersson, R., Niehorster, D. C., & Hooge, I. (2017). Searching for monocular microsaccades – A red Hering of modern eye trackers? *Vision Research*, *140*, 44–54. https://doi.org/10.1016/j.visres.2017.07.012

Otero-Millan, J., Macknik, S. L., Langston, R. E., & Martinez-Conde, S. (2013). An oculomotor continuum from exploration to fixation. *Proceedings of the National Academy of Sciences of the United States of America*, *110*(15), 6175–6180. https://doi.org/10.1073/pnas.1222715110

Otero-Millan, J., Macknik, S. L., & Martinez-Conde, S. (2012). Microsaccades and blinks trigger illusory rotation in the "rotating snakes" illusion. *The Journal of Neuroscience: The Official Journal of the Society for Neuroscience*, *32*(17), 6043–6051. https://doi.org/10.1523/JNEUROSCI.5823-11.2012

Poletti, M., & Rucci, M. (2016). A compact field guide to the study of microsaccades: Challenges and functions. *Vision Research*, *118*, 83–97. https://doi.org/10.1016/j.visres.2015.01.018

Scudder, C. A. (1988). A new local feedback model of the saccadic burst generator. *Journal of Neurophysiology*, *59*(5), 1455–1475. https://doi.org/10.1152/jn.1988.59.5.1455

Steinman, R. M. (1965a). Effect of Target Size, Luminance, and Color on Monocular Fixation*. *JOSA*, *55*(9), 1158–1164. https://doi.org/10.1364/JOSA.55.001158

Steinman, R. M. (1965b). Effect of Target Size, Luminance, and Color on Monocular Fixation*. *Journal of the Optical Society of America*, *55*(9), 1158. https://doi.org/10.1364/JOSA.55.001158

Sylvestre, P. A., & Cullen, K. E. (2002). Dynamics of Abducens Nucleus Neuron Discharges During Disjunctive Saccades. *Journal of Neurophysiology*, *88*(6), 3452–3468. https://doi.org/10.1152/jn.00331.2002

Troncoso, X. G., Macknik, S. L., Otero-Millan, J., & Martinez-Conde, S. (2008). Microsaccades drive illusory motion in the Enigma illusion. *Proceedings of the National Academy of Sciences of the United States of America*, *105*(41), 16033–16038. https://doi.org/10.1073/pnas.0709389105

Valsecchi, M., & Gegenfurtner, K. R. (2015). Control of binocular gaze in a high-precision manual task. *Vision Research*, *110*, 203–214. https://doi.org/10.1016/j.visres.2014.09.005

van der Geest, J. N., & Frens, M. A. (2002). Recording eye movements with video-oculography and scleral search coils: A direct comparison of two methods. *Journal of Neuroscience Methods*, *114*(2), 185–195. https://doi.org/10.1016/S0165-0270(01)00527-1

Van Horn, M. R., & Cullen, K. E. (2012). Coding of microsaccades in three-dimensional space by premotor saccadic neurons. *The Journal of Neuroscience: The Official Journal of the Society for Neuroscience*, *32*(6), 1974–1980. https://doi.org/10.1523/JNEUROSCI.5054-11.2012

Van Horn, M. R., Mitchell, D. E., Massot, C., & Cullen, K. E. (2010). Local Neural Processing and the Generation of Dynamic Motor Commands within the Saccadic Premotor

Network. *The Journal of Neuroscience*, *30*(32), 10905–10917. https://doi.org/10.1523/JNEUROSCI.0393-10.2010

Van Horn, M. R., Waitzman, D. M., & Cullen, K. E. (2013). Vergence neurons identified in the rostral superior colliculus code smooth eye movements in 3D space. *The Journal of Neuroscience: The Official Journal of the Society for Neuroscience*, *33*(17), 7274–7284. https://doi.org/10.1523/JNEUROSCI.2268-12.2013

Waitzman, D. M., & Oliver, D. L. (2002). Midbrain. In V. S. Ramachandran (Ed.), *Encyclopedia of the Human Brain* (pp. 43–68). Academic Press. https://doi.org/10.1016/B0-12-227210-2/00208-9

Winterson, B. J., & Collewijn, H. (1976). Microsaccades during finely guided visuomotor tasks. *Vision Research*, *16*(12), 1387–1390. https://doi.org/10.1016/0042-6989(76)90156-5

Winterson, B. J., & Collewun, H. (1976). Microsaccades during finely guided visuomotor tasks. *Vision Research*, *16*(12), 1387–1390. https://doi.org/10.1016/0042-6989(76)90156-5

Wong, C. K., Ziaks, L., Vargas, S., DeMattos, T., & Brown, C. (n.d.). Sequencing and Integration of Cervical Manual Therapy and Vestibulo-oculomotor Therapy for Concussion Symptoms: Retrospective Analysis. *International Journal of Sports Physical Therapy*, *16*(1), 12–20.

Yu, X., & Lewis, E. R. (1989). Studies with spike initiators: Linearization by noise allows continuous signal modulation in neural networks. *IEEE Transactions on Biomedical Engineering*, *36*(1), 36–43. https://doi.org/10.1109/10.16447

Zhang, H., & Gamlin, P. D. R. (1998). Neurons in the Posterior Interposed Nucleus of the Cerebellum Related to Vergence and Accommodation. I. Steady-State Characteristics.

*Journal of Neurophysiology*, *79*(3), 1255–1269.

https://doi.org/10.1152/jn.1998.79.3.1255

## SUPPLEMENTARY FIGURE

| Characteristic | Binocularity Index | | | | Amplitude | | | |
|---|---|---|---|---|---|---|---|---|
| Comparison | **Coil: Near vs far** | VOG: near vs far | Near: Coil vs VOG | Far: Coil vs VOG | **Coil: Near vs far** | VOG: near vs far | Near: Coil vs VOG | Far: Coil vs VOG |
| 3Dboard | 1 | 1 | 1 | 1 | 1 | 1 | 0 | 1 |
| 2Dboard | 0 | 1 | 0 | 0 | 0 | 0 | 1 | 1 |
| Brock string | 1 | 1 | 1 | 1 | 1 | 1 | 1 | 1 |
| Magic eye | 0 | 0 | 0 | 0 | 0 | 0 | 0 | 0 |
| Depth illusion | 1 | 1 | 0 | 1 | 1 | 0 | 1 | 1 |

**Figure: Binocularity index distribution comparisons across all conditions of near vs far and VOG vs eye coil, 1 indicating significant difference, 0 indicating no statistical difference. Unpaired 2-tailed t-tests were used to look at the differences in binocularity and amplitude between conditions.**